Md. Saiful Islam, Cristiano M.B. Cordeiro, Marcos A.R. Franco, Jakeya Sultana, Alice L.S. Cruz, and Derek Abbot

Terahertz optical fibers [Invited]

Optics Express, 2020; 28(11):16089-16117

DOI: http://dx.doi.org/10.1364/OE.389999

Review Vol. 28, No. 11 / 25 May 2020 / Optics Express 16089
Optics EXPRESS

Terahertz optical fibers [Invited]

MD. SAIFUL ISLAM,[1] CRISTIANO M. B. CORDEIRO,[2,*] MARCOS A. R. FRANCO,[3] JAKEYA SULTANA,[1] ALICE L. S. CRUZ,[3] AND DEREK ABBOTT[1]

[1]School of Electrical & Electronic Engineering, University of Adelaide, SA 5005, Australia
[2]Institute of Physics, Universidade Estadual de Campinas - UNICAMP, Campinas 13083-859, Brazil
[3]Institute for Advanced Studies - IEAv, Sao Jose dos Campos 12.228-001, Brazil
[*]cmbc@ifi.unicamp.br

Abstract: Lying between optical and microwave ranges, the terahertz band in the electromagnetic spectrum is attracting increased attention. Optical fibers are essential for developing the full potential of complex terahertz systems. In this manuscript, we review the optimal materials, the guiding mechanisms, the fabrication methodologies, the characterization methods and the applications of such terahertz waveguides. We examine various optical fiber types including tube fibers, solid core fiber, hollow-core photonic bandgap, anti-resonant fibers, porous-core fibers, metamaterial-based fibers, and their guiding mechanisms. The optimal materials for terahertz applications are discussed. The past and present trends of fabrication methods, including drilling, stacking, extrusion and 3D printing, are elaborated. Fiber characterization methods including different optics for terahertz time-domain spectroscopy (THz-TDS) setups are reviewed and application areas including short-distance data transmission, imaging, sensing, and spectroscopy are discussed.

1. Introduction

Terahertz regime in the electromagnetic spectrum lies midway between microwaves and visible light [1,2], loosely covering the frequency range 0.1–10 THz or wavelengths between 3 mm to 30 μm. The advance of terahertz technology and the growing interest in applications have increased the demand for developing new sources, detectors, waveguides, and other components for efficient control of terahertz waves. Low loss and low dispersion waveguides represent one of the critical technologies for a new generation of terahertz systems. The focus on terahertz has increased because of the recent availability of convenient sources and detectors, bridging the so-called "terahertz gap" that was traditionally due to the lack of practical, low-cost and efficient components. The new frontier includes exciting applications such as non-destructive testing (NDT), label-free and non-invasive molecular detection, detection of DNA hybridization, pharmaceutical drug testing, and broadband short-range communications [3–13]. Terahertz also has potential for biomedical spectroscopy with a photon energy that is lower than that of mid-IR radiation, yet with stronger polar molecular interactions than microwave radiation [14–34]. Moreover, it is in demand for defense and security screening as it can easily penetrate plastics, cardboard and clothing [35]. Despite all the potential applications, terahertz is still in the development phase because most present terahertz systems are bulky and typically depend on free-space transmission. Whilst the availability of sources and detectors has enabled recent work in this area, other components remain primitive in comparison to their optics counterparts (i.e., designed for visible and infrared).

Terahertz radiation is highly sensitive to the atmosphere due to water vapor content. The free space transmission of terahertz experiences various undesirable losses due to the coupling with atmospheric components that significantly reduces the transmission efficiency. Therefore, in order to upgrade some terahertz systems, it is necessary to build up low loss waveguides. As a primary

#389999 https://doi.org/10.1364/OE.389999
Journal © 2020 Received 18 Feb 2020; revised 21 Apr 2020; accepted 23 Apr 2020; published 13 May 2020

Optics EXPRESS

solution, prior studies have proposed several waveguides including metallic wires, parallel plates, dielectric tubes with metal coating, polystyrene foams, sub-wavelength fibers, Bragg fibers, hollow-core fibers, porous-core fibers, and anti-resonant terahertz fibers [3 –176]. Metal wires were proposed in the early days of terahertz technology development [3,36,113]. Single metal wire can operate as a waveguide for terahertz pulses with reduced dispersion and low attenuation [4,115]. However, the coupling of the free-space terahertz beam to the metal wire-guided mode is very ineffective, since the fundamental mode of metal wire waveguide is radially polarized while the photoconductive antennas produce linearly polarized terahertz signal [115]. Two-wire waveguides gained attention with low loss and improved coupling properties [4], however, not practical for real-world applications. In spite of metallic wires possessing desirable propagation characteristics, the most promising device for guiding terahertz is a dielectric waveguide and its principal category is the terahertz optical fiber. Since the introduction of the solid dielectric rod, there are now a large number of proposed designs for terahertz optical fibers—the most advanced designs are based on the concept of specialty optical fibers [4]. Terahertz optical fibers have, for example, the potential to be designed to allow waveguiding through air and much deeper control of the waveguide optical properties such as loss, birefringence, dispersion, transmittance bands, modal areas, etc.

In this review paper, we aim to combine the recent development of terahertz optical fibers with different geometries and guiding mechanisms, the background materials, the fabrication and measurement techniques, and potential applications. The manuscript is organized as follows: section two outlines the optimal materials for terahertz applications, section three outlines different terahertz optical fiber geometries and their guiding mechanisms, sections four and five address the possible fabrication and characterization mechanisms, section six discusses the potential applications, section seven addresses the future prospects of terahertz optical fiber and, finally, this will be followed by a conclusion.

2. Optimal materials for terahertz applications

The background material to build a terahertz waveguide plays an essential role in obtaining a low loss waveguide. Therefore, careful attention must be taken in considering the bulk material during a terahertz fiber design. Recent terahertz studies on different glasses and polymers demonstrate

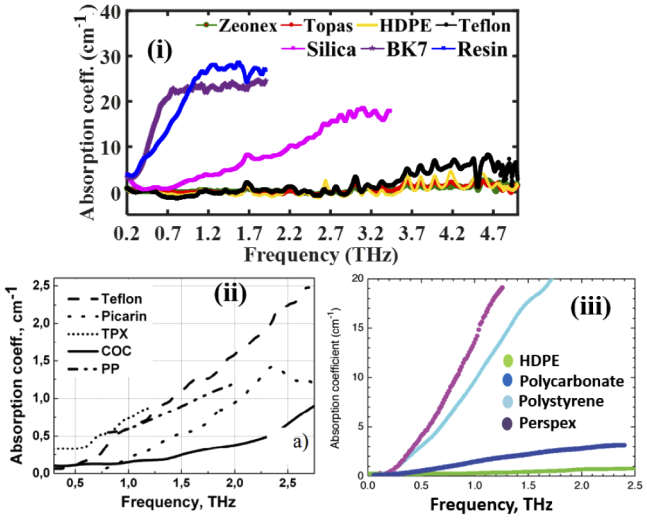

Fig. 1. Absorption coefficients of materials at terahertz, (i) Zeonex, Topas, HDPE, Teflon, Silica, BK7 and uv-resin [177,178], (ii) Teflon, Picarin, TPX, COC, and PP [179], and (iii) HDPE, polystyrene, polycarbonate, and perspex (PMMA) [180,181].

Optics EXPRESS

that polymers show better optical properties than glasses [123,177,178]. From a very recent study of materials for terahertz fibers [177], Fig. 1(i), it was found that the cyclo olefin polymer (COP) (commercially known as Zeonex), cyclic olefin co-polymer (COC) (commercially known as Topas), Teflon, and HDPE show similar optical characteristics. Their absorption coefficient has an average value of 0.2 cm^{-1} in the 0.2 to 5.0 THz [177,178]. At high frequencies, however, Zeonex and Topas present lower losses than Teflon and HDPE [177]. Another study, Fig. 1(ii), shows that COC has lower absorption coefficients than Teflon, Picarin, TPX, and PP (Polypropylene) [179]. Naftaly *et al.* [180] demonstrates that HDPE shows lower absorption than polystyrene, polycarbonate, and perspex (Fig. 1(iii)). From Fig. 1(i), we find that, among the glasses the silica shows lower absorption that is the most used material to fabricate fibres applicable in the optical regime. Note that UV-resin is a typical material used in stereolithography (SLA) printing. It provides higher resolution in printing however with much higher loss compared to Zeonex and Topas. Therefore, from the terahertz optical properties of glasses, polymers, and UV-resin, it can be concluded that polymers have lower absorption coefficients than others where Zeonex and Topas perform better [177,178].

3. Terahertz optical fiber categories and guiding mechanisms

In this section, the main advances in the development of terahertz waveguides are summarized. A large variety of terahertz waveguide concepts have been proposed in the last two decades and, usually, are based on metal wires and dielectric waveguides. As a classical optical fiber, the terahertz wave propagation in dielectric waveguides can be supported by the following physical mechanisms: the total internal reflection effect (TIR) [38], the modified total internal reflection (mTIR) [39] in microstructured fibers (or Photonic Crystal Fiber-PCF), the photonic bandgap effect (PBG) [40], the anti-resonant effect with inhibited coupling of core and cladding modes [41] and the topological channel effect in helically twisted structures [42]. The TIR and mTIR effects are related to the refractive index contrast between core and cladding of an optical fiber, allowing the fiber to propagate electromagnetic waves at the high index core. The mTIR is essentially the same TIR physical effect and is present when the cladding is a microstructured region with lower refractive index material formed by low index inclusions (usually air holes) in the background fiber material [43]. The PBG effect in microstructured optical fibers leads to a condition where the electromagnetic wave is not allowed to propagate in the transverse directions but is able to propagate longitudinally at a defect region [40]. The defect region is a perturbation in the periodic microstructure of the cladding and defines the fibre core region [40]. In this condition, the electromagnetic wave can be guided via an "out-of-plane"photonic bandgap and low loss longitudinal transmission occurs in spectral bands where the two-dimension microstructured lattice exhibits forbidden wavelengths for transverse electromagnetic waves [40,43,44]. These narrow spectral bands depend on the periodic cladding structure, geometry, and refractive index contrast between the background material and the low index periodic inclusions in the microstructured cladding [43,44]. The PBG effect allows wave propagation in hollow-core waveguides that opens the possibility of applications in telecommunications and sensing [43–45].

Some hollow-core PCFs have a cladding microstructure with a high air filling factor (thin webs between large air-holes). This lattice structure is called *kagome* and it does not support the PBG effect. An optical fiber with kagome cladding lattice exhibits a lower density of photonic states and, in this situation, core and cladding modes can coexist without coupling [4,46–49] (guidance based on inhibited coupling). The probability of core and cladding modes to couple depends on the match of their effective indexes and their spatial mode overlap [46]. The low density of cladding modes is a critical condition, reducing the probability of core and cladding mode coupling. This opens the possibility of low loss core guidance in wide spectral range in *kagome* lattice fibers [49].

Optics EXPRESS

In such structures, the cladding is formed by a complex lattice of air-holes with high filling factor, and the fiber core is surrounded by a thin dielectric ring [45–49]. If we consider simplifying this structure to a thin dielectric ring surrounding the hollow-core, this is called a tube fiber (or pipe fiber). Like a kagome structure, the very low density of modes supported by the ring reduces the probability of coupling in core and cladding modes (inhibited coupling). In fact, it is possible to analyze the guidance condition in the tube fiber considering the structure as an anti-resonant reflecting optical waveguide (ARROW) [47]. As a double-layered Fabry-Perot resonator, at the anti-resonant wavelengths the constructive interference occurs inside the hollow-core supporting terahertz transmission, and at the resonant wavelengths the light couples to lossy modes inside the dielectric ring [45–48].

This guidance mechanism is known as the *anti-resonant* effect with inhibited coupling and has been explored in terahertz waveguide design with low loss and wideband transmission. A new guidance effect was recently demonstrated in coreless PCF with a helical twist [42]. The twisted structure presents a topological channel that creates favorable guidance conditions. The helical twist causes a quadratic increase in the optical path as a function of fibers radius and twist rate, impacting more strongly the effective indexes of cladding modes with field distribution far from the fiber center. As a result, a helical twist causes a decoupling (or an inhibited coupling) between modes with field close to the fiber center from modes with field far from the fiber center. The result is a waveguide with low confinement loss, even when the structure is a coreless microstructured fiber [42,52]. Figure 2 presents one example of terahertz optical fiber structure to each possible guidance mechanism.

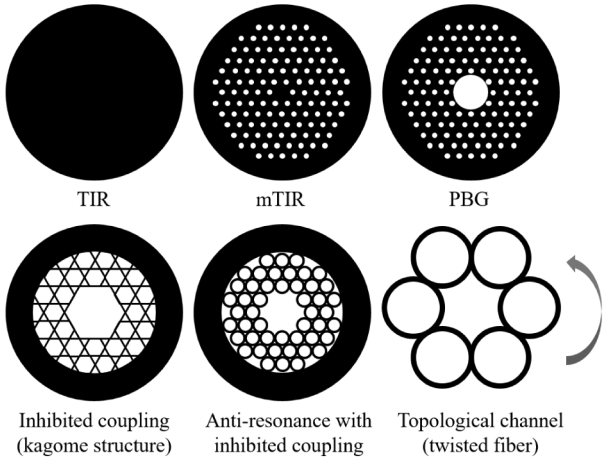

Fig. 2. Representative sketches of terahertz optical fibers with corresponding guidance mechanism indicated.

Terahertz optical fibers have been proposed in the literature building upon the developments in specialty optical fibers [4,53,54]. The designs have explored almost all the guidance mechanisms already applied in photonics. The main categories of terahertz optical fibers are: solid rod fiber (or microwire fiber) [4,53], porous fiber [53–57], porous-core fiber [58–60], slotted core fiber [10,62–64], suspended core fiber [74,94], hollow-core fiber [95–99], hollow-core fiber based on anti-resonances and inhibited coupling mechanism [41,100–106], Bragg fiber [57,101,108,109], porous fiber with embedded metallic wires [37,110–112], and helically twisted fiber [129]. Figure 3 presents the variety of terahertz optical fibers presented in the literature, where black and white colors represent the dielectric material and the air region, respectively.

The main problem in the development of terahertz optical fibers is the strong absorption of terahertz in dielectric (polymers or vitreous) materials. As discussed in Section 2, polymers

Optics EXPRESS

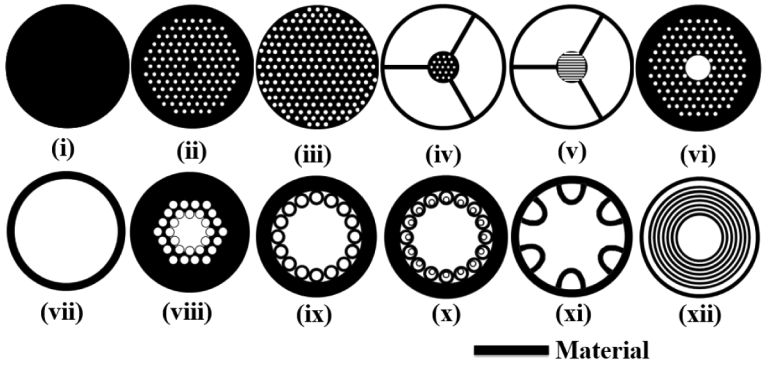

Fig. 3. Optical fiber categories. (i) solid rod fiber, (ii) Microstructured optical fiber, (iii) Porous fiber, (iv) Suspended porous-core fiber, (v) Suspended slotted core fiber, (vi) Hollow-core bandgap fiber, (vii) Hollow-core tube fiber, (viii) Hollow-core fiber with negative curvature, (ix) Hollow-core fiber based on anti-resonances and inhibited coupling, (x) Hollow-core nested anti-resonant nodeless fiber, (xi) 3D printed hollow-core fiber based on anti-resonances and inhibited coupling, and (xii) Bragg fiber.

show low absorption losses than glasses [177]. The high absorption loss demands specialized designs to achieve the desired properties for terahertz optical fibers. A solid rod fiber, the most straightforward terahertz fiber, has high confinement of modal power at the dielectric material, resulting in very high absorption loss. Microstructured solid core terahertz fibers have a similar issue resulting in high absorption losses. However, a coreless porous terahertz fiber with subwavelength air-holes, can reduce the absorption loss by adjusting the fraction of modal power at the air (air-holes plus air-cladding) and at the dielectric background material [56,57]. Porous terahertz fibers reaching 85% of modal core power fraction were demonstrated in [53–57], resulting in reduced propagation losses.

Porous-core terahertz fibers are those in which a dielectric core has a microstructure of subwavelength air-holes and the surrounding cladding is built with larger air-holes [58–61]. Porous-core terahertz fiber provides high confinement with low loss terahertz propagation. However, some designs add extra effort to prepare the fiber preform by including air-holes with very different diameters to build the microstructured core and cladding regions. This kind of porous-core terahertz fiber was proposed in [59,60] leading to high power confinement at the porous-core (40%–40%) region and propagation losses of about 0.07 cm^{-1}. Porous-core fiber design based on the PGB effect allows the use of similar air-hole diameters. This approach was firstly demonstrated in terahertz fibers built with cyclic olefin copolymer (COC–TOPAS) operating at 0.75–1.05 THz with losses lower than 1.5 dB/cm [58]. An even more difficult design was proposed in a porous-core fiber with elliptical air-holes that was proposed to obtain high birefringence of about 0.119 and low-loss propagation of 0.0689 cm^{-1} at the 1.0 THz [68]. In general, a core porosity of 50% to 60% allows reduction of the absorption loss to 45% and 38% of the bulk material loss, respectively [59].

An alternative design to porous-core terahertz fiber is the slotted-core terahertz fiber developed with the purpose of providing high birefringence of about 0.02 to 0.075 at 1 THz [10,62–64] and low loss below 0.06 cm^{-1}[10,148]. Basically, fiber core has high porosity due to the inclusion of rectangular or elliptical slots filled with air [10,62–64]. Slotted-core fibers were only numerically studied because the extra challenge of preparing the fiber preform and integrating rectangular or elliptical slots at the core region into a cladding with circular air-hole macrostructure [10,62–64,148]. Note that Figs. 4(a)–(d) present examples of porous-core and slotted-core terahertz optical fiber designs and their material absorption loss as function of core-diameter and

Optics EXPRESS

porosity [59,148]. Slotted-core terahertz fibers have the potential to result very low propagation losses, but experimental demonstration must be presented.

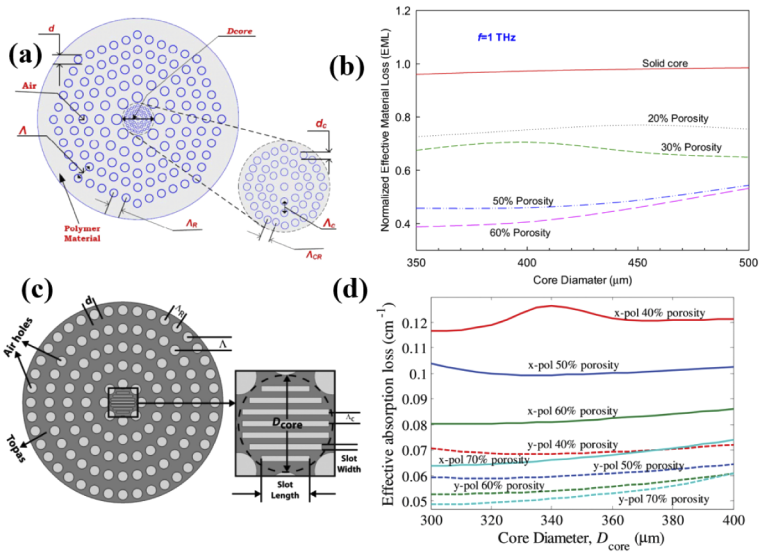

Fig. 4. Porous-core and slotted-core terahertz optical fiber designs and absorption loss as function of core diameter and porosity. (a)-(b) Microstructured porous-core terahertz fiber design and its absorption loss [59]. (c)-(d) Sloted-core terahertz fiber design and its absorption loss [148].

Another category of terahertz fiber is the suspended core fibers that are characterized by a central very small fiber core surrounded by a large porous outer cladding. The fiber core can be solid, hollow-core or microstructured, as a porous-core fiber, and the main characteristic of this kind of terahertz fiber is the high intensity of evanescent field around the core [74,149–151]. An experimental demonstration of suspended-core (150 μm) subwavelength terahertz fiber was presented in [74] with guidance from 0.28–0.48 THz with low-loss of 0.02 cm^{-1}. The main features of this low-loss fiber design is mechanical flexibility, allows ease of fabrication and has a fiber core isolated from external disturbances—this allows convenient hand manipulation that is useful to real world applications. Other suspended-core designs were numerically proposed and a combination of techniques to increase the core porosity and reduce the propagation losses were explored: hollow-core [149,150], slotted-core [151], and graded porous-core [74] (Figs. 5(a)–(d)). However, the increase of design complexity of these alternative designs is an issue that invariably leads to not practical and cost-effective devices.

An optimized design of porous terahertz fiber, or suspended core terahertz fiber can reduce the absorption loss to less than 1/10 of the bulk material loss. However, considering the high absorption losses of dielectric materials, a hollow-core fiber seems to be a more effective option. Based on the established hollow-core fibers for phonics applications in the optical regime, hollow-core terahertz fibers have been proposed based on different guiding mechanisms: the bandgap effect, low cladding mode density in fibers with kagome structure and the anti-resonant effect [41,95–104].

Hollow-core terahertz fibers, based on kagome structures, were demonstrated with remarkable low absorption losses of 0.6 cm^{-1} over 0.65–1.0 THz [97] and 0.02 cm^{-1} over 0.2–1.0 THz, with minimum of 0.002 cm^{-1} at 0.75 THz [98]. The kagome terahertz fiber presented in [97] was fabricated by the stack and draw technique and resulted in single-mode operation with propagation loss about twenty times lower than the loss of polymer PMMA used as manufacture material.

Optics EXPRESS

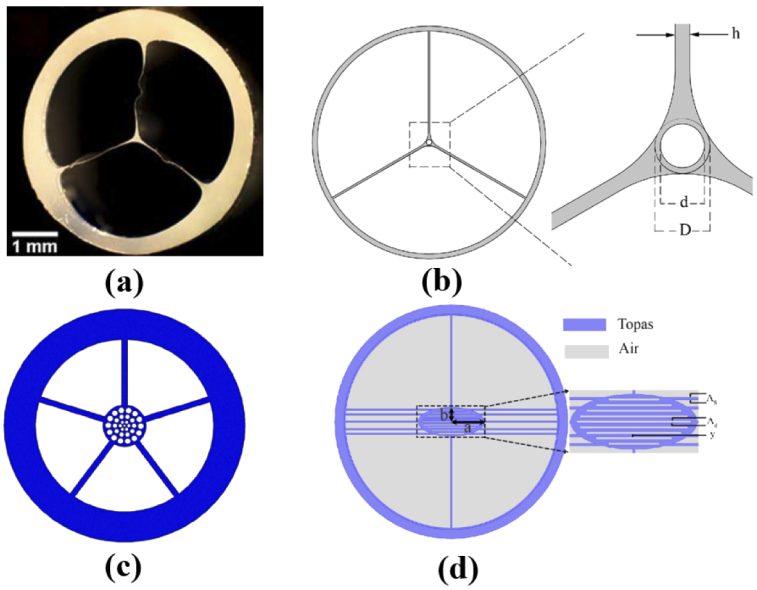

Fig. 5. Suspended-core terahertz fibers. (a) Subwavelength core [74]. (b) Hollow-core [149]. (c) Graded porous-core [74]. (d) Slotted-core [151].

The hollow-core kagome structure presented in [98] was manufactured by 3D printing leading to broadband propagation (above 0.4 THz) and enables mechanical splicing by connecting separated parts without any additional alignment issue. Figures 5(a)–(d) present both kagome based hollow-core fibers and their spectral propagation losses [97,98]. These hollow-core structures are representative of two most promising fabrication techniques applied to terahertz optical fiber manufacture. The first technique (stack and draw) allows obtaining flexible single-mode waveguides and the second technique (additive manufacturing by 3D printing in polymer) open the possibility to fabricate special designs that are impossible to by prepare with any other manufacturing technique.

Despite the efficacy of low-loss PBG and kagome based hollow-core terahertz fibers, a simpler design is even possible and has been explored for terahertz wave propagation. Anti-resonant hollow-core terahertz fibers (tube terahertz fibers) enable wave propagation with extremely low absorption losses of 0.0005 cm^{-1} at 1.0 THz [99,152] over large bandwidths. An anti-resonant waveguide can be formed by just one dielectric tube or a design based on connected tubes as presented in Figs. 6(a) and 6(c). These waveguides present wider transmission bands than that of PBG based hollow-core terahertz fibers. Figures 6(b) and 6(d) present the attenuation constant and loss coefficient to the single tube waveguide and tube lattice waveguide, respectively [99,152].

Besides the search of appropriated designs to obtain low loss terahertz propagation, the another very important parameter to enable broadband terahertz transmission is the chromatic dispersion of terahertz optical fibers. A very simple anti-resonant terahertz fiber, based on just one dielectric tube with absorptive cladding, might provide low loss (0.05–0.5) cm^{-1} and low dispersion propagation ($|\beta_2|$<10 ps/THz/cm) in 0.3–1.0 THz [100]. The authors demonstrated that an absorptive material, placed outside the dielectric tube, reduces the slope of dispersion curves especially in the vicinity of resonant loss maxima, what causes a strong reduction in the group velocity dispersion (GVD), reduction of bending losses (remains <0.2 $cm^{-1}$for bending radii down to 10 cm) and propagation bandwidth much larger that the classical ARROW waveguide [100].

Optics EXPRESS

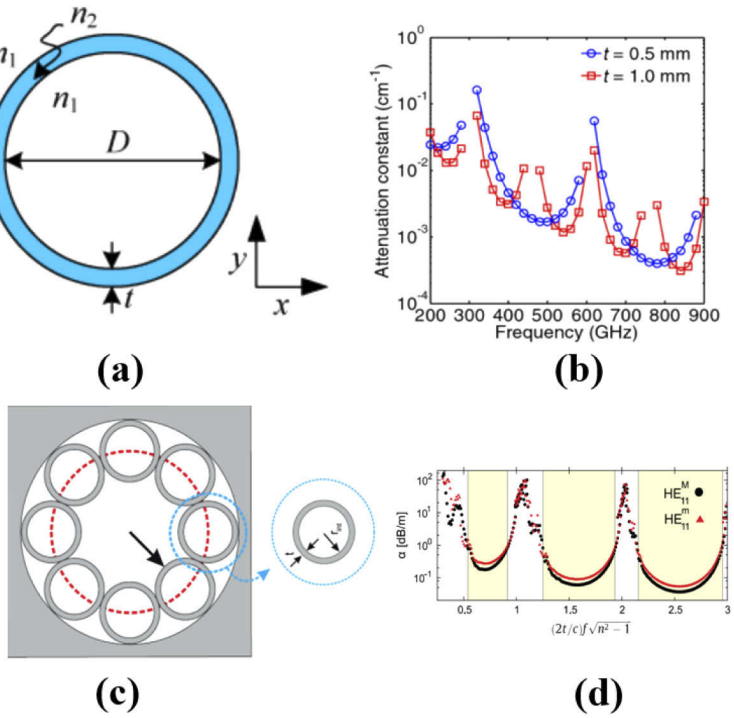

Fig. 6. Hollow-core terahertz fiber based on anti-resonant effect. (a-b) Simplest dielectric tube terahertz waveguide [99]. (c-d) Negative curvature hollow-core tube lattice terahertz waveguide [152].

Another possible design of hollow-core fiber is the Bragg terahertz fiber that consists of a hollow-core surrounded by circular concentric rings of high and low refractive indexes (Bragg reflector). In this category of fiber, usually the fiber core is much larger than the operating wavelength what ensures high coupling efficiency with different terahertz sources [57]. Few studies about Bragg terahertz fibers are available in the literature [57,108,109], but the numerical and experimental results demonstrate transmission from 0.2–2.0 THz and loss of 0.1 cm^{-1} to 1.0 THz [108,109]. Figures 7(a) and (b) present a terahertz Bragg fiber design, manufactured by rolling two different polymer films, and its spectral transmission loss, respectively [108]. This design and manufacture process has the advantage of simplicity, cost effective, besides enable flexible waveguides and propagation from 0.2–2.0 THz. Figures 7(c) and (d) show a 3D printed terahertz Bragg fiber, with diameter core of 7.2 mm, and its spectral transmission loss, respectively [109]. The 3D printed Bragg fibers in low-cost printers, as presented in [109], are also very simple to be fabricated, but the low spatial printing resolution and the use of only one printing material limits the designs to achieve the operation in Bragg regime. An alternative would be filling the air gap with a liquid polymer or another dielectric where the high-index contrast leads to omnidirectional reflection.

An alternative design of hollow-core terahertz fiber is a hybrid terahertz fiber that is based on porous fiber with embedded metallic wires [37,106,110,112]. More details about terahertz fibers with embedded wires will be presented in the next section.

A new frontier of terahertz fiber optic development is the proposal of helically twisted hollow-core terahertz fibers. Considering the new features demonstrated by this category of fibers in photonic applications, there is a significant opportunity to develop devices to manipulate terahertz modes with circular polarization and modes with orbital angular momentum (OAM) [129].

Optics EXPRESS

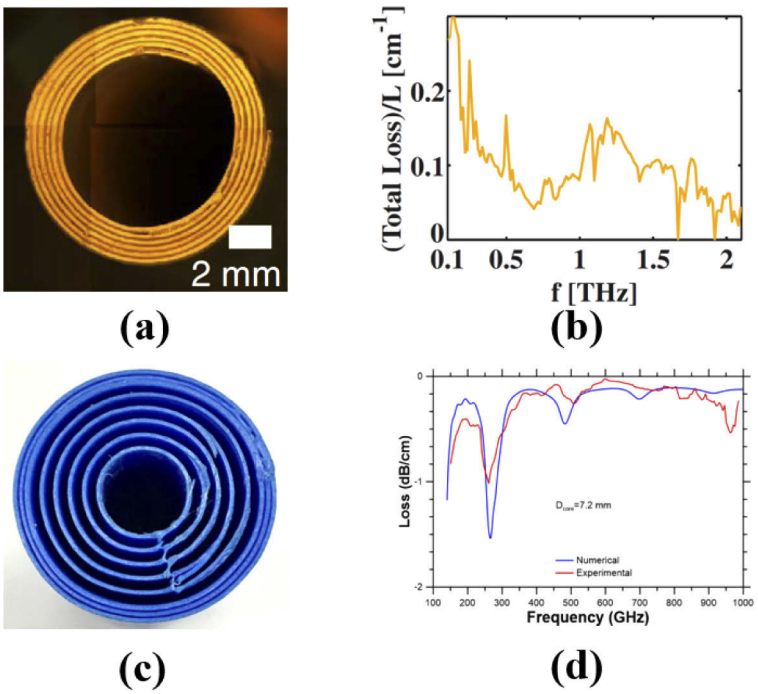

Fig. 7. Hollow-core terahertz Bragg fiber, design and its spectral transmission loss. (a)-(b) Manufactured by rolling two polymer layers [108]. (c)-(d) Fabricated by 3D printing [109].

3.1. Hollow-core waveguides having single and hybrid cladding

In this section, various hollow-core metallic single and hybrid cladded waveguide are discussed. The single clad waveguide refers to a structure with a single layer of material (metal or polymer) (Fig. 8(i)); whereas hybrid clad (metamaterial) waveguides contain a minimum of two different materials, creates conjugate layers (Figs. 8(ii)–(viii)) [37,106,110,112]. The net idea is to combine the low-loss, low-dispersion terahertz propagation properties of metal wires/sheet based waveguides with the mechanical robustness of porous terahertz fibers.

3.1.1. Hollow-core single-clad metallic pipe waveguides

In 1999, McGowan *et al.* reported the first experimental investigation on a long circular stainless-steel hollow pipe waveguide [113]. The next year, Gallot *et al.* extended the idea by reporting a brass circular hollow waveguide [3]. In all of these cases, the terahertz transmission is limited not only by the high loss of the metal but also by group velocity dispersion of the guided waves. Hadika *et al.* [144] in 2005 developed a flexible, hollow terahertz waveguide and compared the results by using both polymer (ferroelectric polyvinylidene fluoride (PVDF)) and metal (copper). An improved loss performance was found by using the polymer than the copper. Alongside the ohmic losses, the inner surface roughness [144] introduced from the washing process and inconsistency of the waveguide cross-section [3] introduced from extrusion over the length are the main limitations of the metal waveguides.

3.1.2. Hollow-core metamaterial waveguides

Hybrid-clad also known as metamaterial waveguide refers to the waveguides having a minimum of two different layers of materials. Each layer has different functionalities, for example, the use of polymer as a supporting tube [110] can introduce the flexibility to deposit metal on polymer

Optics EXPRESS

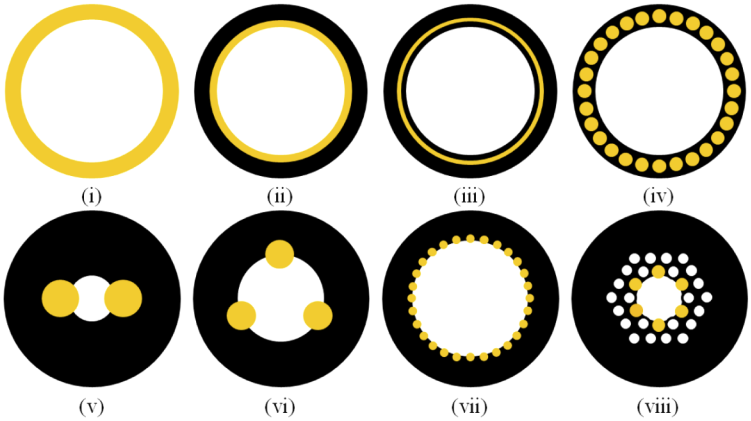

Fig. 8. Hollow core terahertz waveguides with metallic wires and coating. (i) Single metallic cladded waveguide, (ii-iii) hybrid cladded waveguide, (iv) metamaterial cladding [121], (v) two-wire dielectric cladding [111,112,114]; (vi) three wire dielectric cladding [37], (vii-viii) cladding with multiple metal wire inclusions [37,111,121].

inner surface. The inner thin metal layer serves as a reflector and maintains the optical properties. In 2004, Harrington *et al.* adapted metal coating idea using liquid-phase chemistry method from the mid-IR region and applied it to the terahertz spectrum [110]. The ejection of a thin metal layer of correct optimal thickness inside and/or outside of the transparent polymer is the main concept of liquid-phase chemistry method. However, this method possesses complex procedures and limits the coating diameter and length. Various hybrid cladded waveguides are shown in Fig. 8.

A 3D printed porous fiber with embedded metallic wires was reported in [37] reaching low-loss absorption coefficients of 0.05 – 0.4 cm^{-1} and close to zero dispersion (Fig. 8(vii)). A challenge of embedded metal wire design is the careful maintenance of inter-wire gaps along the fiber length, because any variation of this distance can increase the radiation losses significantly [112]. Anthony *et al.* in 2013 analysed two-wire and four-wire configuration of metamaterial waveguide [111]. The reported power loss was 0.3 cm^{-1} for the two-wire fiber, and 0.5 cm^{-1} for the four-wire fiber. To obtain the desired wire-based hybrid cladding geometries, the dielectric waveguide preform can be made first and then metal wires can be inserted manually [37].

The dielectric coating on metal is another type of metamaterial waveguide that facilitates the transmission over a metallic tube waveguide. For example, polystyrene coated metal enhances the reflectivity of the metal via an interference effect and the metal acts as a mirror. An experimental characterization on a silver/polystyrene-coated hollow glass waveguide [116,118] shown that the transmission loss reduces to 0.95 dB/m, in contrast to the high loss of 3.5–5.0 dB/m for the metal-only waveguides. This is due to the low extinction coefficient [119] and low dielectric absorption [120] of the dielectric loaded waveguide. A drawback of introducing the dielectric layer in a metallic waveguide is that the dielectric coating introduces interference peaks, which limits the bandwidth of operation [119]. Thus, the thickness of the dielectric should be optimized in such a way that a low transmission loss window can be located in the desired frequency region. The addition of a thin dielectric layer of an oversized waveguide can reduce losses but enlarging the core size increases the number of modes so that modal coupling and modal dispersion become problematic. A single layer of subwavelength metal wires with optimal thickness is sufficient to provide the required guidance through hollow-core with dielectric cladding environment [121]. The waveguide reported by Li *et al.* was fabricated using co-drawing technique [122] with indium

Optics EXPRESS

wires and Zeonex. Within the single-mode window, the propagation loss of their waveguide is as low as 0.28 dB/cm.

For the wire-based hybrid clad hollow waveguide, the dominant guided mode is a HE11-like mode [37,111]. It should be noted that coated dielectric layer thickness plays an important role in defining the dominant mode between HE11 and TE01. It is found that for correct optimal thickness the dominant mode for the dielectric coated metal waveguide is the HE11 mode [116,117,119,120]. The loaded dielectric film reduces the loss of TM mode, which is higher for the metal waveguide. This results in the dominant mode for the dielectric loaded waveguide to be the HE11 mode with a lower attenuation constant. Table 1 summarizes the main features of terahertz optical fiber categories and address selected works representing the advances in terahertz dielectric waveguides development.

Table 1. Terahertz optical fibers main features.

Terahertz fiber categories	Highlights	Concerns	Extra comments
Solid core, [4,53,155]	Design simplicity, ease of manufacture.	High absorption and bending losses, High dispersion (GVD).	Tapered subwavelength fiber to evanescent field sensing, can be flexible.
Porous [4,53–60,62–67, 135,139]	Average absorption loss and design and manufacture complexity, mechanical robustness.	High bending loss, high dispersion (GVD), multimode guidance.	Tapered subwavelength fiber to evanescent field sensing.
PCF [53,68–71,137]	Mechanical robustness, average design and manufacture complexity, single-mode guidance.	High absorption and bending loss.	Solid, porous or slotted core
Suspended core [11,64,72–74,94]	Reduced absorption loss, Isolated fiber core, High evanescent field into the air cladding, Single-mode guidance.	Design and manufacture with average complexity.	Solid, porous or slotted core Special design to guide with near-zero dispersion.
PBG and kagome hollow-core [71,75,76,95–99]	Reduced absorption and bending losses, Low dispersion.	Design and manufacture complexity, Reduced manufacturing tolerance, Multimode guidance, Large outer diameter.	Bandgap guidance of PBG fiber, wideband guidance of kagome fiber, terahertz signal well coupled to large core diameters.
Anti-resonant [77,100–107]	Low absorption loss, Design simplicity, Ease of manufacture.	Weak mechanical robustness, Multimode guidance.	Single tube fiber, absorptive cladding, terahertz signal well coupled to large core diameters, possible manufacture with 3D printing.
Bragg [57,78,96,101, 108,109]	Reduced absorption loss, Isolated fiber core.	Average manufacture complexity, Reduced manufacturing tolerance, Multimode guidance.	Possible manufacture with 3D printing, terahertz signal well coupled to large core diameters.
Hollow-core with hybrid metallic-dielectric cladding [79–82,106,107, 110–112,114,116, 117,119–122,135]	Low absorption loss, High field confinement in a wide frequency range.	Design and manufacture with high complexity, Reduced manufacturing tolerance.	Low-loss air-bound ARROW modes at high frequencies, close-to-zero dispersion with two-wire configuration, Plasmonic modes at lower frequencies, possible use of embedded metal wires or layers in different fiber designs.

Optics EXPRESS

Table 2 presents selected experimentally demonstrated terahertz optical fibers with description of fiber category, background material, core diameter, effective material loss (EML in cm^{-1}) or confinement loss (CL in dB/cm), and dispersion (GVD). The material abbreviations means: Polystyrene (PE), polypropylene (PP), polymethyl methacrylate (PMMA), polytetrafluoroethylene or teflon (PTFE), cyclic olefin copolymer (COC), cyclo-olefin polymer (COP), VeroWhitePlus (photopolymer), Somos EvoLVe 128 (photopolymer), acrylonitrile butadiene styrene (ABS), polylactic acid (PLA), high-density polyethylene (HDPE), Silica (SiO2), arsenic sulfide (As2S3), high resistivity silicon (HRS).

Table 2. Selected experimentally demonstrated terahertz optical fibers.

Terahertz fiber categories	Material	Core dia. (μm)	Loss (EML or CL)	Dispersion	Reference (year)
Solid core	PE	200	0.01 cm^{-1} at 0.3 THz	-	[135] (2006)
Solid core	PS, COP	1600×1600	0.3 cm^{-1} (PS) and 0.04 cm^{-1} (0.12 THz)	-	[84] (2019)
Porous	Silica	182	1.2-2.0 dB/cm (0.4-0.6 THz)	-	[67] (2006)
Porous	PE	350	0.01 cm^{-1} at 0.3 THz	-	[139] (2009)
Porous	PMMA	200–600	0.25 cm^{-1} at 0.8 THz	-	[65] (2009)
Porous	PE	445, 695	<0.02 cm^{-1} (0.1–0.5 THz)	<1 ps/THz/cm (0.1 – 0.5 THz)	[83] (2010)
Porous	PTFE	430	<0.27 cm^{-1} (0.1–1.0 THz)	-	[85] (2019)
PCF	PTFE	1000	<0.12 cm^{-1} (0.1–1.3 THz)	-	[137] (2004)
PCF	COC	870, 4200	0.09 cm^{-1} (0.35–0.65 THz)	<1 ps/THz/cm	[69] (2009)
Suspended	PE	150	0.02 cm^{-1} (0.28–0.48 THz)	-	[74] (2011)
Kagome	PMMA	1600, 2200	0.8 cm^{-1} (0.75–1.0 THz)	-	[97] (2011)
Kagome	VeroWhite	9000	0.02 cm^{-1} (0.2–1.0 THz)	-	[98] (2016)
Anti-resonant	PTFE	2100	0.05 dB/cm	-	[77] (2013)
Anti-resonant	PMMA	4000	0.05–0.5 cm^{-1} (0.3–1.0 THz)	<10 ps/THz/cm, <1 ps/THz/cm	[100] (2015)
Anti-resonant	Resin	9000×4500	0.005 cm^{-1}	-	[86] (2019)
Anti-resonant	PLA	25000	0.005 cm^{-1}(0.1 THz)	-	[87] (2019)
Anti-resonant	Resin	5000	0.11 cm^{-1}(0.2–1.0 THz)	-	[88] (2020)
Bragg	PTFE	6700	0.001 cm^{-1} (1.0 THz)	-	[108] (2011)
Bragg	ABS	7200	0.52 dB/cm (0.35 THz)	-	[109] (2015)
Bragg	PMMA	4500	0.12 cm^{-1} (0.18 THz)	-	[166] (2017)
Hybrid (metal)	COC	2000	0.2 cm^{-1} (>0.85 THz)	<5 ps/THz/cm (0.65-1.05 THz)	[111] (2013)

Table 3 presents selected numerically studied terahertz optical fibers with description of fiber category, background material, core diameter, effective material loss (EML in cm^{-1}) or propagation loss (dB/cm)propagation loss, and dispersion (GVD).

Optics EXPRESS

Table 3. Selected numerically studied terahertz optical fibers.

Terahertz fiber categories	Material	Core dia. (μm)	Loss (EML or CL)	Dispersion (ps/THz/cm)	Reference (year)
Porous	COC	560, 600, 760	0.007 cm^{-1} (0.2 THz)	-	[62] (2009)
Porous	PMMA	400	0.01 cm^{-1} (0.2 THz)	-	[66] (2008)
Porous	COP	300×400	0.06 cm^{-1} (0.2 THz)	±0.02	[89] (2018)
PCF porous core	COC	350–500	0.1 – 0.2 cm^{-1}(0.7–1.2 THz)	-	[56] (2013)
PCF porous core	COC	350	0.07 cm^{-1}(1.0 THz)	-	[59] (2013)
PCF porous core	COC	200	0.05-0.14 cm^{-1}(0.7-1.6 THz)	1–2.7(0.7–1.6 THz)	[94] (2016)
PCF slotted core	COC	350	0.07 cm^{-1}(1.0 THz)	<4 (0.8–1.3 THz)	[148] (2015)
PCF porous core	COC	450	0.024-0.46 cm^{-1}(1.0 THz)	0.15 (1.0–1.5 THz)	[90] (2017)
PCF porous core	COC	350–500	0.02 cm^{-1}(0.98–1.64 THz)	0.16(1.0–1.58 THz)	[91] (2017)
PCF porous core	COC	350–400	0.04 cm^{-1}(1.0 THz)	0.10 (0.9–1.1 THz)	[92] (2017)
PCF porous core	COC	137–142	0.06 cm^{-1}(1.0 THz)	-	[68] (2017)
PCF porous core	COC	290×870	0.06 cm^{-1}(1.0 THz)	0.03 (1.0–1.8 THz)	[13] (2018)
PCF porous core	HRS	100	0.04 cm^{-1}(0.9–1.0 THz)	0.6 (0.8–1.1 THz)	[14] (2018)
PCF porous core	COC	400	0.34 cm^{-1}(1.0 THz)	0.38 (0.72–2 THz)	[15] (2018)
PCF porous core	COC	350×116	0.07 cm^{-1}(1.0 THz)	1.1 (0.8–1.2 THz)	[16] (2018)
PCF porous core	COC	350	0.02–0.05 cm^{-1}(0.5–1.8 THz)	0.53 (0.5–1.5 THz)	[10] (2018)
PCF porous core	COC	396–408	0.003–0.05 cm^{-1}(1.0 THz)	0.01 (0.97–1.09 THz)	[17] (2018)
PCF porous core	COC	130–225	0.07 cm^{-1}(1.20 THz)	1.2 ± 0.32 (1.1–1.5 THz)	[18] (2019)
PCF slotted core	COC	150–750	0.053 cm^{-1}(1.0 THz)	±0.32 (1.0 THz)	[19] (2019)
PCF slotted core	COC	350	0.07 cm^{-1}(1.0 THz)	4 (0.8–1.3 THz)	[151] (2014)
PCF porous core	COC	300–450	0.053 cm^{-1}(1.0 THz)	-	[76] (2009)
Suspended porous core	COC	432	0.01–0.1 cm^{-1}(0.35 – 1.0 THz)	0.14 (0.7–0.9 THz)	[74] (2019)
Suspended slotted core	COC	320	0.39 dB/cm (0.95 THz)	0.5 (0.7–0.9 THz)	[64] (2018)
Kagome	PTFE	4200	0.023 cm^{-1} (2.1 THz)	0.03 (1.2–2.9 THz)	[71] (2009)
Kagome porous core	COC	300	0.029 cm^{-1} (1.30 THz)	0.49 (1.0–1.76 THz)	[20] (2019)
Kagome porous core	COP	300–400	0.05 cm^{-1} (1.0 THz)	0.49 ± 0.05 (0.8–1.7 THz)	[6] (2018)
Kagome porous core	COP	250–350	0.04 cm^{-1} (1.0 THz)	0.98 ± 0.09 (1.0–2.0 THz)	[93] (2019)
PBG	PTFE, HDPE	882	0.01 dB/cm (0.9–1.1 THz)	-	[76] (2009)
PBG	COP	1500 × 2034	0.01 cm^{-1} (0.82–1.05 THz)	0.16–1.12 (0.82–1.05 THz)	[21] (2018)
PBG	PTFE, PMMA, SiO_2	960-1020	0.0001–0.001 cm^{-1} (1.73 THz)	close to zero (1.6–1.8 THz)	[75] (2019)
Anti-resonant	PMMA	7000, 9000	0.0007–0.004 cm^{-1} (0.7 THz)	-	[99] (2009)
Anti-resonant	PTFE	2100	0.05 dB/cm	-	[77] (2013)
Anti-resonant	PC	6000, 10000	<0.01 dB/cm (0.45 THz)	-	[127] (2018)
Anti-resonant	COC	3000	0.05 dB/cm (0.60 THz)	0.1 (0.8–1.4 THz)	[102] (2018)
Anti-resonant	PP	1300	0.17 cm^{-1} (2.1 THz)	0.1 (0.8–1.4 THz)	[22] (2018)
Anti-resonant	COC	3625	<0.021 dB/cm (2.2 THz)	-	[23] (2018)
Hybrid (metal)	PE	200	0.64 cm^{-1}(>1.514 THz)	2-3 (0.3–0.55 THz)	[79] (2013)
Hybrid	COC	1000	0.25 dB/cm (0.3–0.46 THz)	-	[80] (2016)
Hybrid (Metamaterial)	COP	3000	0.01 dB/cm (1.0 THz) (Center of bandgap)	-	[107] (2020)

Optics EXPRESS

4. Terahertz polymer optical fibers fabrication methods

Fabrication constraints are crucial when designing and developing a new polymer optical fiber. Polymers are considered as the most efficient material for manufacturing terahertz waveguides as they can show low loss and flat dispersion properties in the terahertz regime. The fabrication processes of terahertz polymer fibers are adapted from the microstructured optical fiber. In general, the microstructured optical fibers can be fabricated by drilling, stacking and drawing, extrusion, casting/molding and solvent deposition, and 3D printing. In this section, we discuss the methodology of these fabrication methods and point out a few practical examples of the same.

4.1. Drilling

The drilling method is widely used to fabricate microstructured and photonic crystal preforms with circular holes. Such preforms need to be subsequently drawn to optical fibers to guide visible and infrared signals. The computer numerical controlled (CNC) drilling machine offers to ability to fabricate complex structured preforms with high precision [132]. It should be noted the need to optimize the drilling parameters such as cutting speed, spindle speed and depth of cut to avoid air hole surface roughness or polymer melting due to high drilling temperature. A detailed drilling procedure has been discussed in [131]. The size of the drill imposes a limitation on the maximum length of the preform and determines the number of holes that can be drilled [132]. To control the system temperature and hole deformation, a liquid coolant is required during drilling. Also, the drill bit has a very short lifetime and frequent replacement makes the whole fabrication process complex and time-consuming. Drilling is not suitable for porous-core and anti-resonant fiber because its geometrical complexity. It is also difficult to maintain the mechanical strength of a thin wall between adjacent air holes in fiber structures with a high air filling fraction [132]. A possible geometry is a Bragg fibre with a larger central hole and small holes forming the concentric layers (Fig. 9(a)).

4.2. Stack and draw

Stacking is another approach for creating hole patterns in a preform [134–137,140,141]. A number of polymer capillaries are stacked manually and bundled together with a polymer jacket to prepare the final preform. The microstructured layers of a suitable preform are fastened together with ordinary thin plastic tubes. A wide range of complex structures with different hole patterns has been made using passive or active pressure. This freedom allows changing the shape of originally circular holes like shown in Fig. 9(b) [128,138,139]. Staking is the most common method for fabricating the preforms for hollow-core fiber and porous fiber with high air proportion. The handmade stacking is very labor-intensive and time-consuming for mass production. However, the limitation in the preform length and drawbacks of drill bit imposed by the drilling method can be overcome by this technique. The maximum achieved porosity with stacking is 8–18% [139]. A more detailed stacking procedure has been discussed in [131].

4.3. Sacrificial-polymer technique

The sacrificial polymer technique is a subtraction process, where the sacrificial rods are stacked in the microstructured mold without touching and co-drawn with polyethylene granules [83,139]. The advantage of this technique is that complete hole collapse during drawing can be removed as the preform contains no holes. The PMMA rods are dissolved in tetrahydrofuran (THF), and the air holes reveal in the fiber. The sacrificial material should have a higher glass transition temperature than casting material. A microstructured sub-wavelength fiber with 29–45% porosity has been possible to fabricate with a fiber length of several meters [83,139]. However, to remove the unwanted material and dry the fiber (few days) requires lengthy post-processing [139].

Optics EXPRESS

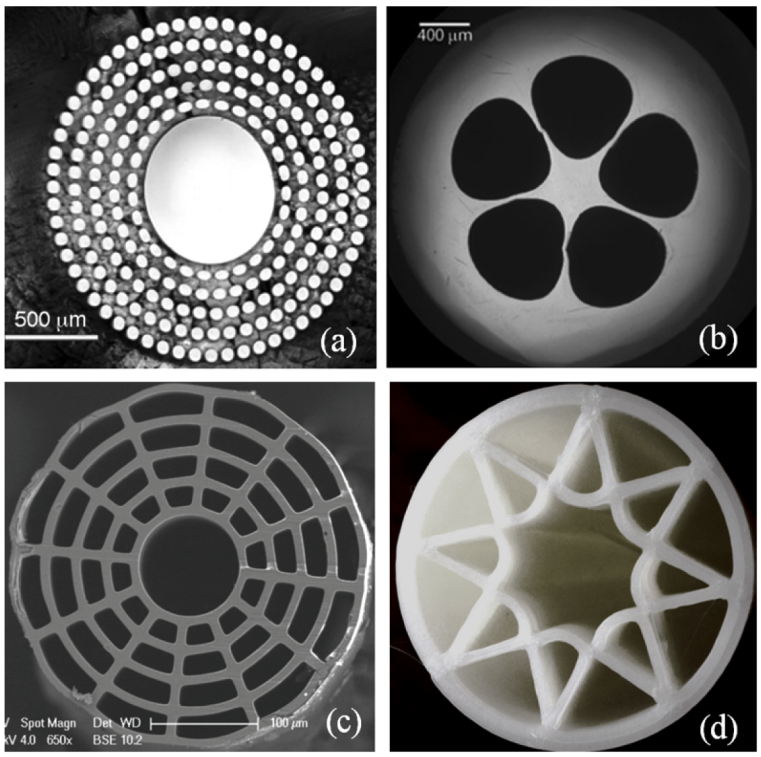

Fig. 9. Terahertz optical fiber fabrication methods. Various geometries of optical fiber fabricated by, (a) drilling [58,123,124,130]; (b) stack and draw [134–137,140,141]; (c) sacrificial-polymer method [83,139], preform-molding/fiber-inflation technique [83,133], and extrusion [55]; (d) 3D printing [105,125,127,142,143].

4.4. Preform-molding/fiber-inflation technique

Molding is a procedure where the fiber preform is cast in a microstructured mold. The microstructured mold features a special structured alignment to assemble a number of polytetrafluoroethylenes coated alloy steel wires [133] or bottom end sealed silica capillaries [83]. The bundle of steel wires/silica capillaries is placed in the bottom end sealed of a large diameter of a quartz tube to enable pressurization in the preform. The tube is filled with polymer granules and placed into a furnace to melt it. Upon cooling, the steel wires/solid rods are removed from the solidified cast preform. The air holes in resultant preform are pressurized to prevent the complete hole collapse during drawing, and the sufficient air pressure inflates the holes with maximum porosity of 86% [83]. The molding technique is suitable for the arbitrary shapes and size in hole patterns by varying the mold structure and arrangement [133]. A drawback of this approach is that the deformation of the porous cross-section can happen with unusual pressurization.

4.5. Extrusion

Extrusion is a common technique to fabricate either the polymer preforms or directly fiber from a billet or from granules. The extrusion dies exit geometry defines the fiber cross-section. Extrusion technique has been applied in microstructured fiber designs named as spider web porous fiber [55], rectangular porous fiber [55], including anti-resonant fiber. The obtainable porosity using extrusion are 57% and 65% [55]. The critical step in extrusion is designing and machining the dies. A new die (or an intensive cleaning process) is required for each extrusion,

Optics EXPRESS

making the fabrication technique expensive and time-consuming. An interesting characteristic is that,different fiber structures can be fabricated using the extrusion technique. Figure 9(c) shows various fibers fabricated using the sacrificial-polymer, preform-molding, and extrusion technique.

4.6. 3D Printing

Note that 3D printing is a well established and comparatively easier method of fabricating terahertz optical fibers. The most widely used 3D printing techniques are stereolithography (SLA) (uses a laser scanner to solidify the liquid resin which are photocurable) [126], fused filament method (FDM) (uses a nozzle to soften Zeonex, Topas, PMMA, PC, PE, ABS, Nylon) [127], polymer jetting technique (uses UV lamps on print heads to cure acrylic polymer and water-soluble polymer layer) [125,142], each of which are suited to a range of terahertz fiber fabrication techniques. An example of an FDM 3D printing sample is shown in Fig. 9(d). The 3D printing process allows preparation in a single-stage process, forming complex fiber geometries without any further processing or drawing. The 3D printing technique allows for rapid prototyping of fiber designs as the fabrication cycle is significantly shorter. The limitation of 3D printing technology is that the choice of material needs to be compromised for improved surface roughness. The use of FDM has the ability to use many different polymers. That comes, however, with higher surface roughness. The SLA technique can improve surface roughness but the choice of material is restricted.

5. Characterization procedures of terahertz waveguides

In this section, two most commonly used measurement systems such as terahertz time-domain spectroscopy (THz-TDS), and continuous-wave terahertz (CW-THz) spectroscopy are discussed as the tool for terahertz waveguide characterization. In THz-TDS, coherent detection of time-domain signal can directly measure the transient electric field that is then Fourier transformed to provide the properties of the sample under study as a function of the frequency. A basic linear THz-TDS consists of a terahertz source (emitter) and terahertz detector, pumped by a femtosecond laser system where terahertz optics (mirrors/lenses) are optional. The three different THz-TDS setups are explored in this review, as illustrated in Fig. 10, and capable of transmission mode measurement.

In the first setup, the input and output faces of waveguide are directly positioned inline to the emitter and detector (Fig. 10(a)). In this case, the terahertz pulse is directly propagate towards the core of the fiber that is then received by the detector. The emitter and detector are the fixed components for the THz-TDS, where the path length between them is altered according to the waveguide length, [55,127]. Generally, large core fibers can be excited directly by solely using the transmitter and receiver, where additional lenses are not required. An alternative approach for waveguide characterization is using mirrors and hyperspherical silicon/polymer lenses at the front and end interface of the waveguide, 10(b). This kind of setup is generally necessary in order to achieve smaller beam size and strong beam coupling with the waveguide. As an example, [3,99,111,113,123–125], uses this method of waveguide characterizations where smaller beam size was required. A similar kind of beam size can be achieved by using four lenses (silicon/polymer) as shown in Fig. 10(c). The lenses in this case need to be positioned and optimized according to their focal length, [182].

Note that CW-THz is another commonly used system for waveguide characterization (Fig. 10(d)). The setup shown in Fig. 10(d) has two distributed feedback lasers that has slightly different center wavelength. The wavelengths are equally distributed to the emitter and detector arm by the 50:50 coupler. The fiber stretchers in this CW-THz system create additional path delay and cancel the phase noise.

Generally, there are two different methods for waveguide characterization. In the first method, measurements of the same sample with different lengths can be carried out by inserting and

Optics EXPRESS

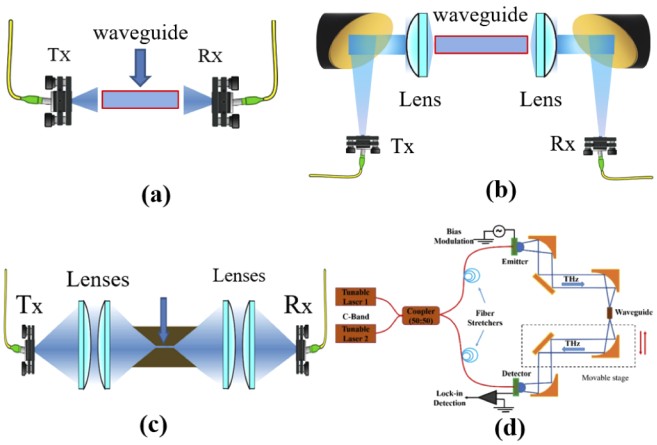

Fig. 10. Characterization methods of terahertz optical fiber. (a) THz-TDS setup where the waveguide placed in between emitter and detector [55,127]; (b) THz-TDS setup by using high resistive silicon lenses [99,113,125], (c) a four lens setup of THz-TDS [182], (d) a CW-THz setup [183].

removing them in the setup [3,113,121]. This method of measurement introduces a coupling loss that varies from measurement to measurement as every time a sample is inserted the beams needed to be re-alignment. Another approach is the cut-back technique, where the waveguide entrance is kept fixed on the setup while the sample has its length shortened and the transmission power measured [110,116,117]. The use of the cutback method is limited to fibers that can be easily cut without being moved out from the characterization setup.

Over the last few years THz-TDS has become a reliable, and commercial available product, however the high cost of the femtosecond laser needed to excite the photoconductive antenna hinders their widespread use for commercial applications [184,185]. One of the advantage of the CW-THz system is their high spectral resolution that depends on laser linewidth. Moreover, the full CW-THz system can be driven by laser diodes that makes the system much more compact and inexpensive [184,185].

Here and in the previous sections, the types of terahertz optical fibers, their guiding mechanisms, suitable materials for terahertz guidance and possible fabrication and characterization methods were discussed. On a general note, we find that loss is a significant issue for terahertz wave propagation, which can be significantly reduced by optimal choice of fiber geometry and background material. One of the main hurdles in the field is the imperfect fabrication of terahertz fibers. For example, 3D printing technology can produce complex fiber structures but, in general, with non-ideal materials and/or with high surface roughness and low transparency. Other processes can be time-consuming or require multiple steps. Some fibers can also be very thick (many mm in diameter) reducing its flexibility or be very fragile making it difficult the cleaving process of a high-quality surface. A practical consequence is an extra effort in doing a cut-back loss measurement and getting reliable experimental coupling and transmission loss data.

6. Applications of terahertz optical fibers

The field of terahertz optical fibers is still in development. The main applications of terahertz fibers include short-distance data transmission, sensing, and imaging. For propagation, terahertz fibers must present low losses, low dispersion and, in some cases, have mechanical flexibility. The principal issue in the realization these fibers is high absorption loss of most materials in the terahertz regime, which implies increased fiber transmission loss. While negligible loss

Optics EXPRESS

materials are not available, one method to overcome and control the losses is via optimization of fiber design. In sensing applications, fibers are used to increase the interaction of terahertz power with the analyte, leading to sensors with higher sensitivity. This interaction may occur outside the fiber, as in rod fibers, or the core of a hollow-core fiber. The use of hollow-core fibers goes beyond refractive index analyses, and has been employed for real-time monitoring and molecular concentration sensors. Moreover, imaging systems employ terahertz fibers as probes to deliver and collect signal dfor biological sensing, for example. All these mentioned applications depend on low loss fibers, thus research effort for overcoming these material losses are critical for real-world applications and continued improvement is expected over the coming years.

6.1. Transmission and communication

The primary use of terahertz optical fibers is to transport T-waves with minimal influence of the external medium. Since the 2000s, significant effort has been carried out in the development of low loss and low dispersion terahertz waveguides to improve fiber transmission properties. The first circular dielectric terahertz waveguide was a solid polymeric rod which guided terahertz waves with an attenuation constant of 0.01 cm^{-1} [145]. To date, several studies have proposed low loss waveguides optimization of fiber design and improved choice of available fabrication materials [57,59,74,146].

A recent study [147] presented a combination of a porous-core circular PCF fabricated with the low loss material, Topas. In this case, 52% of the power fraction was present in the microstructured core region, which reduces the overlap between the terahertz modal power and the host material. This effect leads to an effective material loss (EML) of (0.034 cm^{-1}) and an ultra-flattened dispersion variation of 0.09 ps/THz/cm (Fig. 11(i)). This numerical approach also showed guiding characteristics such as single mode propagation and birefringence. Generally, these propagation characteristics are required for transmission and communication applications. In 2019, a suspended graded-index porous-core fiber was proposed [74] (Fig. 11(ii)). The guiding mechanism is based on TIR, and the numerical where numerical investigation shows that by introducing a graded-index in the fiber core an extremely flat dispersion of 0.14 ± 0.07 ps/THz/cm and an intermodal dispersion of 0.0152 ± 0.0004 ps/THz/cm are achieved. These dispersion values were found over 0.75 to 1.0 THz when the fiber core diameter is 432 μm. An asymmetrical terahertz fiber was also reported [9] (Fig. 11(iii)), with a high fiber birefringence of 0.063, an EML of 0.06 cm^{-1} and nearly zero dispersion flattened property of ± 0.02 ps/THz/cm. The anti-resonant hollow-core terahertz fiber [102] (Fig. 11(iv)) is also a promising candidate for low loss terahertz transmission. An investigation on this type of fiber shows a loss of 0.05 dB/m and 600 GHz wide dispersion flattened bandwidth [102]. Based on the results above, it is possible to find out a promising path to guide terahertz waves in short and long distances. Although these designs were investigated only numerically, the authors rely on the available fabrication methods discussed in Section 4 for practical applications.

6.2. Sensing

As in the optics regime, terahertz fibers can also be used for sensing applications to detect substances as liquids, vapors, solid particles or thin material layers. Terahertz rod fibers, or subwavelength rod fibers, for example, guide electromagnetic waves with a frequency dependent high power fraction due to the infinite air cladding. The evanescent field is sensitive to changes in the cladding refractive index, shifting the waveguide dispersion curve. As an example, in 2009, a liquid sensor based on a polystyrene wire was demonstrated. In the experiment, water and alcohol were readily distinguished and a variation of 58% in the dispersion curve between those two liquids was observed. Moreover, melamine and polyethylene alcohol solutions were investigated. It was observed that by increasing the melamine and PE concentrations from 0 ppm to 100 ppm, a change in the dispersion curve occurred up to the solution saturation limit,

Optics EXPRESS

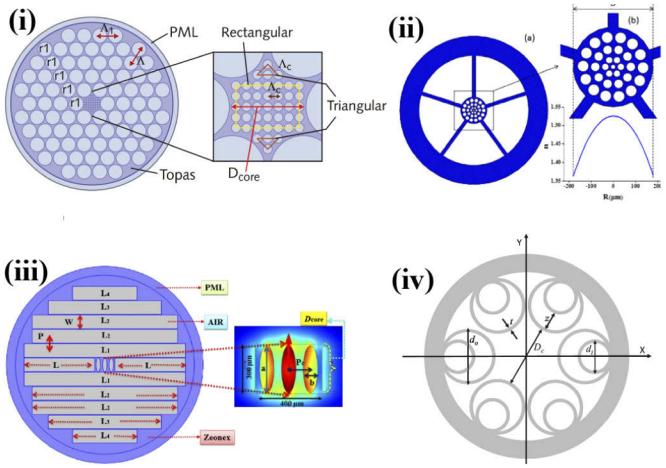

Fig. 11. Low losses Terahertz optical fibers. (i) PCF like fiber with microstructured core [147]. (ii) Graded-index core fiber [74]. (iii) Asymmetrical terahertz fiber [9]. (iv) Antiresonant terahertz fiber [102].

80 ppm for melamine and 40 ppm for PE [158]. The sensor was able to detect variations of 20 ppm in the solution concentration, equivalent to refractive index changes of 0.01. Also, based on a solid core fiber, a numerical study showed an interferometric fiber sensor for terahertz frequencies [153]. The sensor was formed by a Singlemode-Multimode-Singlemode structure, and the operation principle was based on multimodal interference in the multimode fiber. A sensitivity of 5 GHz.RIU over a refractive index range of 1.4–1.5 was obtained. Apart from the chemical sensors listed, several sensing schemes based on Bragg gratings have also been proposed for strain sensing [154], distributed sensing [155], and thickness monitoring [156].

Terahertz Bragg fibers also have been used as sensors [157,166]. Cao *et al.* [157] showed an interesting result regarding a 3D printed terahertz Bragg fiber as a resonant fluidic sensor. There, a modal analysis for the rectangular Bragg fiber (Fig. 12(i)) was numerically studied with a defective layer located in the reflective Bragg structure. This layer simulates the region filled by the fluid analyte to be characterized. The spectral changes in the resonant absorption peaks were investigated as a function of fluid RI using a continuous-wave terahertz spectroscopy system. An sensitivity of 110 GHz/RIU was achieved (Fig. 12(ii)). A study by Li *et al.* [166] showed the application of a 3D printed terahertz Bragg fiber as a powder and thin-film sensor with sensitivity close to 0.1 GHz/μm.

Hollow-core fibers and hollow-tubes present resonant characteristics in its spectral transmission. Many sensors in the optical and terahertz regimes have been proposed based on anti-resonant mechanism. The resonant peaks present in the waveguide spectral transmission are sensitive to refractive-index variations inside and outside the core, leading to shifts in their resonant frequency. For powder and vapor detection, for example, a glass tube waveguide was presented by You *et al.* [159], where, the hollow-tube was filled with ammonia, acetone, HCl, and water separately. The changes in the tube spectral transmission showed a limit of molecular density around 1.6 nano-mole/mm^3 and sensitivity around 22.2 GHz/RIU. Other work [160] demonstrated a hollow-tube based sensor to analyze subwavelength-thick molecular overlayers in the fiber core. The lowest thickness detectable was about 2.9 μm of aqueous concentrations of carboxy polymethylene powder (carbopol) [160]. Plasmonic fiber [161], sapphire fiber [162] and a large number of numerical studies have shown promising fiber designs for sensing of alcohol and petroleum derivatives [32,163], chemical agents [29,32,163,164], for example, but further practical results on fiber sensing applications are still needed.

Optics EXPRESS

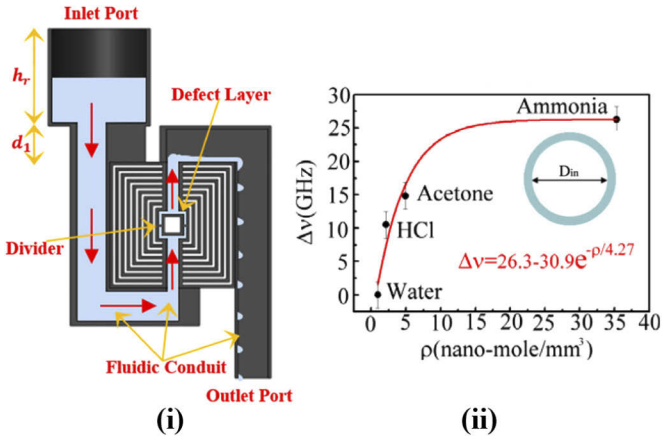

Fig. 12. Application of terahertz optical fiber in sensing and imaging. (i) Micro-fluid sensor based on 3D printed Bragg fiber [74,166]; (ii) Sensitivity of the pipe sensor to different samples: water, HCl, acetone and ammonia [159].

6.3. *Fiber-based terahertz imaging*

A considerable number of terahertz imaging and spectroscopy systems were demonstrated over the last twenty years [74,147,165,167]. Among the different approaches to near-field imaging [167], fiber-scanning systems have been proposed as a powerful option to non-destructive testing, investigation of concealed objects, and endoscopy. In 2008, Lu *et al.* [168] proposed a terahertz scanner using a subwavelength plastic fiber as a probe. The imaging system consisted of a polyethylene solid core fiber, a continuous wave Gunn oscillator, and a Golay cell. In this system, one end of the fiber was free to move, and the other end was fixed. This configuration was suitable for scanning a 6×6 cm^2 area, and allowed measuring the terahertz transmission through transparent samples, such as dry seahorses and fishes, and concealed objects (Fig. 13).

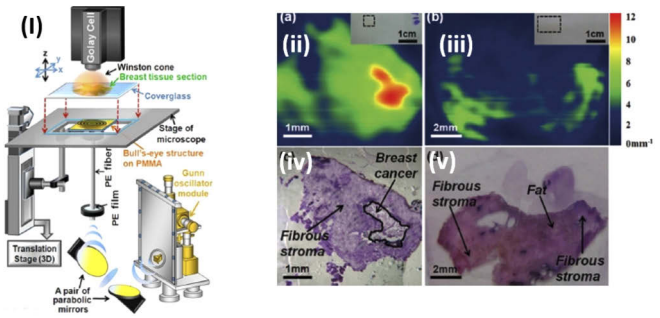

Fig. 13. Schematic of the all-terahertz fiber scanning near-field microscope. Here, (ii) and (iii) are terahertz near-field absorption coefficient images of the breast tissue sections, cancerous and normal samples, respectively. Also, (iv) and (v) are photomicrographs of the corresponding breast tissue.

A study on fiber based terahertz near field microscopy was carried out to diagnose breast tumors [169] where the bulls eye corrugated structure designed to enhance the spatial resolution. This imaging system was capable of being interconnected with an optical microscope, and samples were able to be observed simultaneously, where images of cancerous cells and healthy tissues could also be distinguished. Based on the same principle, equivalent systems were used

Optics EXPRESS

to diagnose breast tumors and liver cancer in [169,170]. A fiber based *in-vivo* detection system of breast cancer was also reported where the system has the ability to detect cancer before it was evident with other techniques [171]. Their study indicates that the system has the potential to be used in a pre-clinical investigation of cancer, and other applications in terahertz microscopy. Other fibers as metamaterial fibers [172] and sapphire fibers [173] have also been studied as potential subdiffraction imaging probes for terahertz near-field systems.

7. Future remarks

Free-space terahertz wave propagation is still widely used, but terahertz waveguides and, in particular, optical fibers are gaining increasing attention. Their importance is related to the concept of developing complex terahertz configurations that potentially combine sources and detectors with a reliable and simple way of terathertz transmission. Many materials and optical fiber geometries have been studied and analyzed and most promising results indicate the use of low loss polymers to manufacture fibers where most of the transmitted power can be guided in air. Anti-resonant fibers stand out among other hollow-core fibers, due to their robustness to fabrication tolerances, geometrical simplicity, and hence fabrication feasibility. Combining simplicity and low attenuation with high bandwidth, single-mode guidance, and low dispersion is, for most applications, the main target. Fibers possessing composite cladding, with metamaterial inclusion, better confine the terahertz signal [121], and fibers with helically twisted to guide modes with orbital angular momentum are two of the most exciting directions for actual and near future investigations.

Different manufacturing techniques are being used to produce such fibers, but 3D printing technology represents a clear advantage in terms of cost, time, easiness, and potential for manufacture of specialty fibers [96] already integrated with other components required for a particular application. The use of filaments, made of low loss polymers (listed in section 3), is required, but they are not always available commercially. Another clear drawback is the poor surface roughness of 3D printed fibers when low-cost desktop printers are used. It should be noted that sophisticate 3D printers able to produce higher quality samples usually require proprietary filaments preventing the direct usage of special polymers. Post-processing a 3D printed fiber is likely an excellent strategy to enhance its quality (roughness, layers adhesion, transparency, etc.). Here we can include the concept already applied to produce 3D printed fibers for the optical and infrared regime [174], i.e., printing a fiber preform and subsequently drawing it to a fiber stage. Extrusion is another powerful technique that is likely to be applied to mass production of high-quality specially designed THz optical fibers. There, the whole fiber cross-section can be produced simultaneously [55]-different from 3D printing or stacking-and-draw, for example. Simple and complex waveguides can be obtained by carefully designing the extrusion die, ram speed and furnace temperature profile. Extrusion of fiber projects with intrinsic low confinement loss due mostly air guidance, and while using low THz loss materials, is an interesting route to be wider explored.

Due to their large overall dimensions, with external diameters as big as 10 mm in some situations [98,175], some terahertz fibers are not mechanically flexible and this reduces the practical interest in applications requiring long waveguide lengths. Investigating ways of producing flexible fibers via selection of the required mechanical properties the fiber material and the fiber geometry (such as fibers with high air filling fraction and thin external jackets), as well as studying waveguide curvature loss will help develop this field further. Combining special coatings such as graphene [176] could extend the functionalities of terahertz fibers and will likely be a hot topic in this vibrant research area.

Terahertz waves have been demonstrated as promising technology to non intrusive analysis in biological, medical, chemical, and industrial applications. However, compact, portable, cost effective and robust devices need to be developed. In this scenario, the terahertz optical fibers,

Optics EXPRESS

usually fabricated in short lengths, represent a challenge and a great opportunity to make such devices a reality.

8. Conclusion

The work on terahertz optical fiber discussed throughout the manuscript combines, the analysis of suitable materials that can be used to make a low loss terahertz optical fiber; a comprehensive review of various geometry including the microstructured photonic crystal fiber, the hollow-core fiber, the antiresonant fiber and the metamaterial-based fibers; the guiding mechanism of each type of fibers; an analysis of different methodology of fiber fabrication and characterization; and finally an outline of suitable application areas with further directions of future work. From the analysis of various glasses and polymers, it has been found that polymers perform better as compared to glasses. From the polymers, the Zeonex, Topas, TPX, Teflon and HDPE show comparatively lower absorption losses and therefore suitable to be considered as a building material of terahertz optical fiber. Various geometries of terahertz optical fibers including their guiding mechanisms have been reviewed and discussed. This fiber includes the hollow pipe waveguides (polymers/metals), microstructured optical fibers including hollow-core and porous-core, the hollow-core photonic bandgap fibers and the antiresonant terahertz fibers. From the discussion, it can be noted that every fiber has some advantages and disadvantages and there is a trade-off between low loss, bandwidth and fabrication feasibility. For example, hollow-core fiber can provide low loss terahertz guidance and comparatively simple fabrication at the expense of low bandwidth of operation. On the other hand, porous fiber can provide larger bandwidth but with higher loss and increased fabrication complexity as compared to hollow-core fibers. Metamaterial-based waveguides are still in their infancy by comparison. The various fabrication methodologies discussed in the manuscript indicate the possibilities of fabricating various geometries of terahertz optical fibers. For example, as discussed in section 6, the drilling method is suitable for fabricating circular hole patterns only, whereas the extrusion and 3D printing technique can fabricate any type of complex and asymmetric fiber geometries. The most common method for terahertz fiber characterization is the use of THz-TDS where different optics setups can be used to focus signal onto the fiber core. Among the various terahertz applications short-range high throughput transmission, gas, and chemical sensing and imaging show significant promise.

Funding

Sao Paulo Research Foundation (FAPESP) (2018/10409-7); Australian Research Council (DP170104981).

Acknowledgments

M. S. Islam coordinates the work to be finalized and writes sections I, II, V, and VIII. C. M. B. Cordeiro writes section VII. M. A. R. Franco writes section III. J. Sultana contributes to section III, and IV. A. L. S. Cruz contributes writing section VI. D. Abbott conceives the idea and approves the manuscript for final submission. All the authors read and review the manuscript before submission.This work was supported in part by the Sao Paulo Research Foundation (FAPESP) under grant 2018/10409-7 and Australian Research Council (ARC) Grant DP-170104981.

Disclosures

The authors declare that there are no conflicts of interest related to this article.

References

1. D. Abbott and X.-C. Zhang, "T-ray imaging, sensing, and retection," Proc. IEEE **95**(8), 1509–1513 (2007).

Optics EXPRESS

2. M. Tonouchi, "Cutting-edge terahertz technology," Nat. Photonics **1**(2), 97–105 (2007).
3. G. Gallot, S. P. Jamison, R. W. McGowan, and D. Grischkowsky, "Terahertz waveguides," J. Opt. Soc. Am. B **17**(5), 851–863 (2000).
4. S. Atakaramians, A. V. Shahraam, T. M. Monro, and D. Abbott, "Terahertz dielectric waveguides," Adv. Opt. Photonics **5**(2), 169–215 (2013).
5. P. H. Siegel, "Terahertz technology in biology and medicine," IEEE Trans. Microwave Theory Tech. **52**(10), 2438–2447 (2004).
6. M. S. Islam, J. Sultana, A. Dinovitser, B. W.-H. Ng, and D. Abbott, "A novel Zeonex based oligoporous-core photonic crystal fiber for polarization preserving terahertz applications," Opt. Commun. **413**(15), 242–248 (2018).
7. M. S. Islam, J. Sultana, S. Rana, M. R. Islam, M. Faisal, S. F. Kaijage, and D. Abbott, "Extremely low material loss and dispersion flattened topas based circular porous fiber for long distance terahertz wave transmission," Opt. Fiber Technol. **34**, 6–11 (2017).
8. M. S. Islam, S. Rana, M. R. Islam, M. Faisal, H. Rahman, and J. Sultana, "Porous-core photonic crystal fiber for ultra-low material loss in terahertz regime," IET Commun. **10**(16), 2179–2183 (2016).
9. M. S. Islam, J. Sultana, A. Dinovitser, B. W.-H. Ng, and D. Abbot, "Zeonex based asymmetrical terahertz photonic crystal fiber for multichannel communication and polarization maintaining applications," Appl. Opt. **57**(4), 666–672 (2018).
10. J. Sultana, Md. S. Islam, M. Faisal, M. R. Islam, B. W. -H. Ng, H. E. Heidepriem, and D. Abbot, "Highly birefringent elliptical core photonic crystal fiber for terahertz application," Opt. Commun. **407**, 92–96 (2018).
11. M. S. Islam, M. R. Islam, M. Faisal, H. Rahman, J. Sultana, and S. Rana, "Extremely low-loss, dispersion flattened porous-core photonic crystal fiber for terahertz regime," Opt. Eng. **55**(7), 076117 (2016).
12. M. S. Islam, M. R. Islam, M. Faisal, H. Rahman, J. Sultana, S. Rana, and M. R. Islam, "Ultra-low loss hybrid core porous fiber for broadband applications," Appl. Opt. **56**(4), 1232–1237 (2017).
13. M. S. Islam, J. Sultana, A. Dinovitser, B. W.-H. Ng, and D. Abbott, "A modified hexagonal photonic crystal fiber for terahertz applications," Opt. Mater. **79**, 336–339 (2018).
14. T. Yang, C. Ding, R. W. Ziolkowski, and Y. J. Guo, "A scalable THz photonic crystal fiber with partially-slotted core that echibits improved birefringence and reduced loss," J. Lightwave Technol. **36**(16), 3408–3417 (2018).
15. E. Reyes-Vera, J. Ú.restrepo, C. Jiménez-Durango, J. M.-Cardona, and N. G.-Cardona, "Design of low-loss and highly birefringent porous-core photonic crystal fiber and its application to terahertz polarization beam splitter," IEEE Photonics J. **10**(4), 1–13 (2018).
16. Md. A. Habib, Md. S. Anower, and Md. R. Hasan, "Highly birefringent and low effective material loss microstructure fiber for THz wave guidance," Opt. Commun. **423**, 140–144 (2018).
17. B. K. Paul, Md. S. Islam, S. Sen, K. Ahmed, and M. S. Uddin, "Low material loss and dispersion flattened fiber for single mode THz-wave transmission applications," Results Phys. **11**, 638–642 (2018).
18. Md. A. Habib and Md. S. Anower, "Design and numerical analysis of highly birefringent single mode fiber in Thz regime," Opt. Fiber Technol. **47**, 197–203 (2019).
19. D.-D. Wang, C.-L. Mu, D.-P. Kong, and C.-Y. Guo, "High birefringence, low loss, and flattened dispersion photonic crystal fiber for terahertz application," Chin. Phys. B **28**(11), 118701 (2019).
20. S. Rana, A. S. Rakin, Md. R. Hasan, Md. S. Reza, R. Leonhardt, D. Abbott, and Harish Subbaraman, "Low loss and flat dispersion kagome photonic crystal fiber in the terahertz regime," Opt. Commun. **410**, 452–456 (2018).
21. H. Xiao, H. Li, B. Wu, and S. Jian, "Polarization-maintaining terahertz bandgap fiber with a quasi-elliptical hollow-core," Opt. Laser Technol. **105**, 276–280 (2018).
22. M. M. Nazarov, A. V. Shilov, K. A. bzheumikhov, Z. C. Margushev, V. I. Sokolov, A. B. Sotsky, and A. P. Shkurinov, "Eight-capillary cladding THz waveguide with low propagation losses and dispersion," IEEE Trans. Terahertz Sci. Technol. **8**(2), 183–191 (2018).
23. S. Yan, S. Lou, X. Wang, T. Zhao, and W. Zhang, "High-birefringence hollow-core anti-resonant THz fiber," Opt. Quantum Electron. **50**(3), 162 (2018).
24. J. Sultana, M. S. Islam, and D. Abbott, "High numerical aperture, highly birefringent novel photonic crystal fibre for medical imaging applications," Electron. Lett. **54**(2), 61–62 (2018).
25. D. M. Mittleman, R. H. Jacobsen, R. Neelamani, R. G. Baraniuk, and M. C. Nuss, "Gas sensing using terahertz time domain spectroscopy," Appl. Phys. B: Lasers Opt. **67**(3), 379–390 (1998).
26. E. Gerecht, K. O. Douglass, and D. F. Plusquellic, "Chirped-pulse terahertz spectroscopy for broadband trace gas sensing," Opt. Express **19**(9), 8973–8984 (2011).
27. H. Lin, W. Withayachumnankul, B. M. Fischer, S. P. Mickan, and D. Abbott, "Gas recognition with terahertz time-domain spectroscopy and spectral catalog: a preliminary study," Proc. SPIE **6840**, 68400X (2007).
28. E. Pickwell and V. P. Wallace, "Biomedical applications of terahertz technology," J. Phys. D: Appl. Phys. **39**(17), R301–R310 (2006).
29. M. S. Islam, J. Sultana, K. Ahmed, A. Dinovitser, M. R. Islam, B. W.-H. Ng, and D. Abbott, "A novel approach for spectroscopic chemical identification using photonic crystal fiber in the terahertz regime," IEEE Sens. J. **18**(2), 575–582 (2018).
30. M. S. Islam, J. Sultana, M. Biabanifard, M. J. Nine, Z. Vafapour, C. M. B. Cordeiro, A. Dinovitser, B. W.-H. Ng, and D. Abbott, "Electrically tunable graphene metasurface for multiband superabsorption and terahertz sensing,"

Optics EXPRESS

44th International Conference on Infrared, Millimeter, and Terahertz Waves (IRMMW-terahertz), 2019, (doi: 10.1109/IRMMW-terahertz.2019.8873851).
31. M. S. Islam, J. Sultana, M. Biabanifard, M. J. Nine, Z. Vafapour, C. M. B. Cordeiro, A. Dinovitser, B. W.-H. Ng, and D. Abbott, "Tunable localized surface plasmon graphene metasurface for multiband superabsorption and terahertz sensing," Carbon **158**, 559–567 (2020).
32. M. S. Islam, J. Sultana, A. A. Rifat, A. Dinovitser, B. W.-H. Ng, and D. Abbott, "Terahertz sensing in a hollow-core photonic crystal fiber," IEEE Sens. J. **18**(10), 4073–4080 (2018).
33. B. S. Williams, "Terahertz quantum-cascade lasers," Nat. Photonics **1**(9), 517–525 (2007).
34. W. L. Chan, J. Deibel, and D. M. Mittleman, "Imaging with terahertz radiation," Rep. Prog. Phys. **70**(8), 1325–1379 (2007).
35. G. E. Tsydynzhapov, P. A. Gusikhin, V. M. Muravev, I. V. Andreev, and I. V. Kukushkin, "New terahertz security body scanner," *43rd International Conference on Infrared, Millimeter, and Terahertz Waves (IRMMW-terahertz)*, 2018, (doi: 10.1109/IRMMW-terahertz.2018.8510513).
36. T.-In Jeon, J. Zhangm, and D. Grischkowsky, "Terahertz sommerfeld wave propagation on a single metal wire," Appl. Phys. Lett. **86**(16), 161904 (2005).
37. N. Yudasari, J. Anthony, and R. Leonhardt, "Terahertz pulse propagation in 3D-printed waveguide with metal wires component," Opt. Express **22**(21), 26042–26054 (2014).
38. G. P. Agrawal, "*Fiber-Optic Communication Systems, Third Edition*," (John Wiley & Sons, Inc., 2002).
39. F. Poli, A. Cucinotta, and S. Selleri, "Photonic crystal fibers properties and applications," (Springer, 2007).
40. J. C. Knight, J. Broeng, T. A. Birks, and P. St. J. Russel, "Photonic band gap guidance in optical fibers," Science **282**(5393), 1476–1478 (1998).
41. L. Vicentti and V. Setti, "Waveguiding mechanism in tube lattice fibers," Opt. Express **18**(22), 23133–23146 (2010).
42. R. Beravat, G. K. L. Wong Michael, H. Frosz, X. M. Xi, and P. St. J. Russel, "Twist-induced guidance in coreless photonic crystal fiber: a helical channel for light," Sci. Adv. **2**(11), e1601421 (2016).
43. P. Russell, "Photonic crystal fibers," Science **299**(5605), 358–362 (2003).
44. J. C. Knight, "Photonic crystal fibres," Nature **424**(6950), 847–851 (2003).
45. A. C. S. Jr, "Recent progress and novel applications of photonic crystal fibers," Rep. Prog. Phys. **73**(2), 024401 (2010).
46. A. Argyros and J. Pla, "Hollow-core polymer fibres with a kagome lattice: potential for transmission in the infrared," Opt. Express **15**(12), 7713–7719 (2007).
47. F. Gérôme, R. Jamier, J.-L. Auguste, G. Humbert, and J.-M. Blondy, "Simplified hollow-core photonic crystal fiber," Opt. Lett. **35**(8), 1157–1159 (2010).
48. F. Couny, F. Benabid, and P. S. Light, "Large-pitch kagome-structured hollow-core photonic crystal fiber," Opt. Lett. **31**(24), 3574–3576 (2006).
49. F. Couny, F. Benabid, P. J. Roberts, P. S. Light, and M. G. Raymer, "Generation and photonic guidance of multi-octave optical-frequency combs," Science **318**(5853), 1118–1121 (2007).
50. F. Yu and J. C. Knight, "Negative curvature hollow-core optical fiber," IEEE J. Sel. Top. Quantum Electron. **22**(2), 146–155 (2016).
51. C. Wei, R. Joseph Weiblen, C. R. Menyuk, and J. Hu, "Negative curvature fibers," Adv. Opt. Photonics **9**(3), 504–561 (2017).
52. P. St. Russel, R. Beravat, and G. K. L. Wong, "Helically twisted photonic crystal fibres," Philos. Trans. R. Soc., A **375**(2087), 20150440 (2017).
53. A. Argyros, "Microstructures in polymer fibres for optical fibres, terahertz waveguides, and fibre-based metamaterials," ISRN Opt. **2013**, 1–22 (2013).
54. A. Barh, B. Pada Pal, G. P. Agrawal, R. K. Varshney, and B. M. Azizur Rahman, "Specialty fibers for terahertz generation and transmission: a review," IEEE J. Sel. Top. Quantum Electron. **22**(2), 365–379 (2016).
55. S. Atakaramians, S. Afshar V., H. E.-Heidepriem, M. Nagel, B. M. Fischer, D. Abbot, and T. M. Monro, "Terahertz porous fibers: design, fabrication and experimental characterization," Opt. Express **17**(16), 14053–14062 (2009).
56. N. Chen, J. Liang, and L.-y. Ren, "High-birefringence, low loss porous fiber for single-mode terahertz-wave guidance," Appl. Opt. **52**(21), 5297–5302 (2013).
57. A. Hassani, A. Dupuis, and M. Skorobogatiy, "Porous polymer fibers for low-loss terahertz guiding," Opt. Express **16**(9), 6340–6351 (2008).
58. H. Bao, K. Nielsen, H. K. Rasmussen, P. U. Jepsen, and O. Bang, "Fabrication and characterization of porous-core honeycomb bandgap terahertz fibers," Opt. Express **20**(28), 29507–29517 (2012).
59. S. F. Kaijage, Z. Ouyang, and X. Jin, "Porous-core photonic crystal fiber for low loss terahertz waveguiding," IEEE Photonics Technol. Lett. **25**(15), 1454–1457 (2013).
60. A. Aming, M. Uthman, R. Chitaree, W. Mohammed, and B. M. Azizur Rahman, "Design and characterization of porous-core polarization maintaining photonic crystal fiber for terahertz guidance," J. Lightwave Technol. **34**(23), 5583–5590 (2016).
61. G. K. M. Hasanuzzaman, Md. S. Habib, S. M. A. Razzak, A. Hossain, and Y. Namihira, "Low loss single-Mode porous-Core kagome photonic crystal fiber for THz wave guidance," J. Lightwave Technol. **33**(19), 4027–4031 (2015).

Optics EXPRESS

62. S. Atakaramians, S. Afshar, V. B. M. Fischer, D. Abbot, and T. M. Monro, "Low loss, low dispersion and highly birefringent terahertz porous fibers," Opt. Commun. **282**(1), 36–38 (2009).
63. A. L. S. Cruz, A. C. C. Migliano, J. G. Hayashi, C. M. B. Cordeiro, and M. A. R. Franco, "Highly birefringent polymer terahertz fiber with microstructure of slots in the core," *22nd International Conference on Plastic Optical Fibers*, (2013).
64. J. Luo, S. Chen, H. Qu, Z. Su Li, and F. Tian, "Highly birefringent single-mode suspended-core fiber in terahertz regime," J. Lightwave Technol. **36**(16), 3242–3248 (2018).
65. S. Atakaramians, S. Afshar V., H. Ebendorff-Heidepriem, M. Nagel, B. M. Fischer, D. Abbot, and T. M. Monro, "THz porous fibers: design, fabrication and experimental characterization," Opt. Express **17**(16), 14053–14062 (2009).
66. S. Atakaramians, S. Afshar V., H. Ebendorff-Heidepriem, M. Nagel, B. M. Fischer, D. Abbot, and T. M. Monro, "Porous fibers: a novel approach to low loss THz waveguides," Opt. Express **16**(12), 8845–8854 (2008).
67. M. Nagel, A. Marchewka, and H. Kurz, "Low-index discontinuity terahertz waveguides," Opt. Express **14**(21), 9944 (2006).
68. K. Ahmed, S. Chowdhury, B. K. Paul, Md. S. Islam, S. Sen, Md. I. Islam, and S. Asaduzzaman, "Ultrahigh birefringence, ultralow material loss porous core single-mode fiber for terahertz wave guidance," Appl. Opt. **56**(12), 3477–3483 (2017).
69. K. Nielsen, H. K. Rasmussen, A. J. L. Adam, P. C. M. Planken, O. Bang, and P. U. Jepsen, "Bendable, low-loss Topas fibers for the terahertz frequency range," Opt. Express **17**(10), 8592–8601 (2009).
70. R. Islam, "Dispersion flattened, low-loss porous fiber for single-mode terahertz wave guidance," Opt. Eng. **54**(5), 055102 (2015).
71. L. Vincentti, "Numericl analysis of plastic hollow core microstructure fiber for terahertz applications," Opt. Fiber Technol. **15**(4), 398–401 (2009).
72. M. Rozé, B. Ung, A. Mazhorova, M. Walther, and M. Skorobogatiy, "Suspended core subwavelength fibers: towards practical designs for low-loss terahertz guidance," Opt. Express **19**(10), 9127–9138 (2011).
73. X. Jiang, D. Chen, and G. Hu, "Suspended hollow core fiber for terahertz wave guiding," Appl. Opt. **52**(4), 770–774 (2013).
74. S. Mei, D. Kong, L. Wang, T. Ma, Y. Zhu, X. Zhang, Z. He, X. Huang, and Y. Zhang, "Suspended graded-index porous core POF for ultra-flat near-zero dispersion terahertz transmission," Opt. Fiber Technol. **52**, 101946 (2019).
75. H. Pkarzadeh, S. M. rezaei, and L. Namroodi, "Hollow-core photonic crystal fibers for efficient terahertz transmission," Opt. Commun. **433**, 81–88 (2019).
76. L. Vicentti, "Hollow core photonic band gap fiber for THz applications," Microw. Opt. Technol. Lett. **51**(7), 1711–1714 (2009).
77. L. Vincetti and V. Setti, "Elliptical hollow-core tube lattice for terahertz applications," Opt. Fiber Technol. **19**(1), 31–34 (2013).
78. Y. Zhang and I. D. Robertson, "Single-mode terahertz Bragg fiber design using a modal filtering approach," IEEE Trans. Microwave Theory Tech. **58**(7), 1985–1992 (2010).
79. A. Markov and M. Skorobogatiy, "Two-wire terahertz fibers with porous dielectric support," Opt. Express **21**(10), 12728–12743 (2013).
80. H. Li, G. Ren, S. Atakaramians, B. T. Kuhlmey, and S. Jian, "Linearly polarized single TM mode terahertz waveguide," Opt. Lett. **41**(17), 4004–4007 (2016).
81. B.-S. Sun, X.-L. Tang, X. Zeng, and Y.-W. Shi, "Characterization of cylindrical terahertz metallic hollow waveguide with multiple dielectric layers," Appl. Opt. **51**(30), 7276–7285 (2012).
82. X. tang, Z. Yu, X. Tu, J. Chen, A. Argyros, B. T. Kuhlmey, and Y. Shi, "Elliptical metallic hollow fiber inner-coated with non-uniform dielectric layer," Opt. Express **23**(17), 22587–22601 (2015).
83. A. Depuis, A. Mazhorova, F. Désévédavy, M. Rozé, and M. Skorobogatiy, "Spectral characterization of porous dielectric subwavelength THz fibers fabricated using a microstructured molding technique," Opt. Express **18**(13), 13813–13827 (2010).
84. R. Guo Eva-Maria Stuebling, F. Beltran-Mejua, D. Ulm, T. Kleine-Ostmann, F. Ehrig, and M. Koch, "3D printed terahertz rectangular waveguides of polystyrene and TOPAS: a comparison," J. Infrared, Millimeter, Terahertz Waves **40**(1), 1–4 (2019).
85. Y. S. Lee, S. Kim, I. Maeng, C. Kang, and K. Oh, "Los-loss terahertz pulse transmission through commercially available porous tubes with PTFE," Proc. SPIE **11206**, 112061S (2019).
86. S. Yang, X. Sheng, G. Zhao, and S. Li, "Simple birefringent terahertz fiber based on elliptical hollow core," Opt. Fiber Technol. **53**, 102064 (2019).
87. S. Li, Z. Dai, Z. Wang, P. Qi, Q. Su, X. Gao, C. Gong, and W. Liu, "Simple birefringent terahertz fiber based on elliptical hollow core," Optik **176**, 611–616 (2019).
88. S. Yang, X. Sheng, G. Zhao, S. Lou, and J. Guo, "Anti-deformation low loss double pentagon nested terahertz hollow core fiber," Opt. Fiber Technol. **56**, 102199 (2020).
89. Md. S. Islam, J. Sultana, A. Dinovitser, M. Faisal, M. R. Islam, B. W.-H. Ng, and D. Abbott, "Zeonex-based asymmetrical terahertz photonic crystal fiber for multichannel communication and polarization maintaining applications," Appl. Opt. **57**(4), 666–672 (2018).
90. Md S. Islam, M. Faisal, and S. M. A. Razzak, "Dispersion flattened porous-core honeycomb lattice terahertz fiber for ultra low loss transmission," IEEE J. Quantum Electron. **53**(6), 1–8 (2017).

Optics EXPRESS

91. Md S. Islam, M. Faisal, and S. M. A. Razzak, "Extremely low loss porous-core photonic crystal fiber with ultra-high dispersion in terahertz regime," J. Opt. Soc. Am. B **34**(8), 1747–1754 (2017).
92. Md. S. Islam, J. Sultana, J. Atai, D. Abbott, S. Rana, and M. R. Islam, "Ultra low-loss hybrid core porous fiber for broadband applications," Appl. Opt. **56**(4), 1232–1237 (2017).
93. J. Sultana, M. R. Islam, M. Faisal, and Md. K. Abu Talha, "Design and analysis of a Zeonex based diamond-shaped core kagome lattice photonic crystal fiber for T-ray wave transmission," Opt. Fiber Technol. **47**, 55–60 (2019).
94. S. Rana, M. S. Islam, M. Faisal, K. C. Roy, R. Islam, and S. F. Kaijage, "Single-mode porous fiber for low-loss polarization maintaining terahertz transmission," Opt. Eng. **55**(7), 076114 (2016).
95. L. Vicentti, "Hollow-core photonic band gap fiber for terahertz applications," Microw. Opt. Technol. Lett. **51**(7), 1711–1714 (2009).
96. A. L. S. Cruz, C. M. B. Cordeiro, and M. A. R. Franco, "3D printed hollow-core terahertz fibers," Fibers **6**(3), 43 (2018).
97. J. Anthony, R. Leonhardt, S. G. L.-Saval, and A. Argyros, "Terahertz propagation in kagome hollow-core microstructured fibers," Opt. Express **19**(19), 18470–18478 (2011).
98. J. Yang, J. Zhao, C. Gong, H. Tian, L. Sun, P. Chen, L. Lin, and W. Liu, "3D printed low-loss terahertz waveguide based on kagome photonic crystal structure," Opt. Express **24**(20), 22454–22460 (2016).
99. C.-H. Lai, B. You, j. Y. Lu, T. A. Liu, J.-L. Peng, C.-K. Sun, and H.-c. Chang, "Modal characteristics of anti-resonant reflecting pipe waveguides for terahertz waveguiding," Opt. Express **18**(1), 309–322 (2010).
100. H. Bao, K. Nielsen, O. Bang, and P. U. Jepsen, "Dielectric tube waveguides with absorptive cladding for broadband, low-dispersion and low loss terahertz guiding," Sci. Rep. **5**(1), 7620 (2015).
101. Y.-F. Zhu, M.-Y. Chen, and Y. Liu, "Nested low-loss hollow-core fiber," IEEE J. Sel. Top. Quantum Electron. **26**(4), 1–6 (2020).
102. G. K. M. Hasanuzzaman, S. Iezekiel, C. Markos, and M. S. Habib, "Hollow-core fiber with nested anti-resonant tubes for low-loss terahertz guidance," Opt. Commun. **426**, 477–482 (2018).
103. A. L. S. Cruz, V. A. Serrao, C. L. Barbosa, C. M. B. Cordeiro, A. Argyros, X. Tang, and M. A. R. Franco, "3D Printed hollow-core fiber with negative curvature for terahertz applications," J. Microw. Optoelectron. Electromagn. Appl. **14**, 45–53 (2015).
104. A. L. S. Cruz, C. M. B. Cordeiro, G. S. Rodrigues, J. H. Osório, L. E da Silva, and M. A. R. Franco, "Exploring terahertz hollow-core fiber designs manufactured by 3Dprinting," *IEEE MTT-S International Microwave and Optoelectronics Conference (IMOC 2017)*, Águas de Lindoia, Brazil (2017).
105. J. Sultana, M. S. Islam, C. M. B. Cordeiro, A. L. S. Cruz, A. Dinovitser, B. W.-H. Ng, and D. Abbott, "Five-Capillary Cladding Terahertz Fiber with Low Loss and Single Mode," *44th International Conference on Infrared, Millimeter, and Terahertz Waves (IRMMW-terahertz)*, 2019. DOI: 10.1109/IRMMW-THz.2019.8874476.
106. J. Sultana, M. S. Islam, C. M. B. Cordeiro, A. L. S. Cruz, A. Dinovitser, B. W.-H. Ng, and D. Abbott, "Novel hollow-core anti-resonant terahertz fiber with metamaterial cladding," *44th International Conference on Infrared, Millimeter, and Terahertz Waves (IRMMW-terahertz)*, 2019. DOI: 10.1109/IRMMW-THz.2019.8873836.
107. J. Sultana, M. S. Islam, C. M. B. Cordeiro, A. Dinovitser, M. Koushik, B. W.-H. Ng, and D. Abbott, "Terahertz hollow core antiresonant fiber with metamaterial cladding," Fibers **8**(2), 14–00 (2020).
108. A. Dupuis, K. Stoeffer, B. Ung, C. Dubois, and M. Skorobogatiy, "Transmission measurements of hollow-core terahertz Bragg fibers," J. Opt. Soc. Am. B **28**(4), 896–907 (2011).
109. A. L. S. Cruz, A. Argyros, X. Tang, C. M. B. Cordeiro, and M. A. R. Franco, "3D-Printed Terahertz Bragg Fiber," *40th International Conference on Infrared, Millimeter and Terahertz Waves (IRMMW 2015)*, Hong Kong, Aug 2015.
110. J. A. Harrington, R. George, and P. Pedersen, "Hollow polycarbonate waveguides with inner Cu coatings for delivery of terahertz radiation," Opt. Express **12**(21), 5263–5268 (2004).
111. J. Anthony, R. Leonhardt, and A. Argyros, "Hybrid hollow-core fibers with embedded wires as terahertz waveguides," Opt. Express **21**(3), 2903–2912 (2013).
112. A. Markov, H. Guerboukha, and M. Skorobogatiy, "Hybrid metal wire-dielectric terahertz waveguides: challenges and opportunities," J. Opt. Soc. Am. B **31**(11), 2587–2600 (2014).
113. R. W. McGowan, G. Gallot, and D. Grischkowsky, "Propagation of ultrawideband short pulses of terahertz radiation through submillimeter-diameter circular waveguides," Opt. Lett. **24**(20), 1431–1433 (1999).
114. A. Markov, S. Gorgutsa, H. Qu, and M. Skorobogatiy, "Practical metal-wire THz waveguides," *arXiv:1206.2984*, 2012.
115. K. Wang and D. Mittleman, "Metal wires for terahertz guiding," Nature **432**(7015), 376–379 (2004).
116. B. Bowden, J. A. Harrington, and O. Mitrofanov, "Silver/polystyrene-coated hollow glass waveguides for the transmission of terahertz radiation," Opt. Lett. **32**(20), 2945–2947 (2007).
117. B. Bowden, J. A. Harrington, and O. Mitrofanov, "Low-loss modes in hollow metallic terahertz waveguides with dielectric coatings," Appl. Phys. Lett. **93**(18), 181104 (2008).
118. B. Bowden, J. A. Harrington, and O. Mitrofanov, "Fabrication of terahertz hollow-glass metallic waveguides with inner dielectric coatings," J. Appl. Phys. **104**(9), 093110 (2008).
119. Y. Matsuura and E. Takeda, "Hollow optical fibers loaded with an inner dielectric film for terahertz broadband spectroscopy," J. Opt. Soc. Am. B **25**(12), 1949–1954 (2008).
120. X.-L. Tang, Y.-W. Shi, Y. Matsuura, K. Iwai, and M. Miyagi, "Transmission characteristics of terahertz hollow fiber with an absorptive dielectric inner-coating film," Opt. Lett. **34**(14), 2231–2233 (2009).

Optics EXPRESS

121. H. Li, S. Atakaramians, R. Lwin, X. Tang, Z. Yu, A. Argyros, and B. T. Kuhlme, "Flexible single-mode hollow-core terahertz fiber with metamaterial cladding," Optica **3**(9), 941–947 (2016).
122. A. Tuniz, R. Lwin, A. Argyros, S. C. Fleming, and B. T. Kuhlmey, "Fabricating metamaterials using the fiber drawing method," J. Visualized Exp. **68**, e4299 (2012).
123. J. Anthony, R. Leonhardt, A. Argyros, and M. C. J. Large, "Characterization of a microstructured Zeonex terahertz fiber," J. Opt. Soc. Am. B **28**(5), 1013–1018 (2011).
124. C. S. Ponseca, R. Pobre, E. Estacio, N. Sarukura, A. Argyros, M. C. J. Large, and M. A. van Eijkelenborg, "Transmission of terahertz radiation using a microstructured polymer optical fiber," Opt. Lett. **33**(9), 902–904 (2008).
125. Z. Wu, W-R. Ng, M. E. Gehm, and H. Xin, "Terahertz electromagnetic crystal waveguide fabricated by polymer jetting rapid prototyping," Opt. Express **19**(5), 3962–3972 (2011).
126. J. Li, K. Nallappan, H. Guerboukha, and M. Skorobogatiy, "3D printed hollow-core terahertz Bragg waveguides with defect layers for surface sensing applications," Opt. Express **25**(4), 4126–4144 (2017).
127. L. D. Van Putten, J. Gorecki, E. Numkam Fokoua, V. Apostolopoulos, and F. Poletti, "3D-printed polymer anti-resonant wave-guides for short-reach terahertz applications," Appl. Opt. **57**(14), 3953–3958 (2018).
128. V. Setti, L. Vincetti, and A. Argyros, "Flexible tube lattice fibers for terahertz applications," Opt. Express **21**(3), 3388–3399 (2013).
129. A. Stefani, S. C. Fleming, and B. T. Kuhlmey, "Terahertz orbital angular momentum modes with flexible twisted hollow-core anti-resonant fiber," APL Photonics **3**(5), 051708 (2018).
130. K. Nielsen, H. K. Rasmussen, A. J. L. Adam, P. C. M. Planken, O. Bang, and P. U. Jepsen, "Bendable, low-loss Topas fibers for the terahertz frequency range," Opt. Express **17**(10), 8592–8601 (2009).
131. E. Arrospide, G. Durana, M. Azkune, G. Aldabaldetreku, I. Bikandi, L. R.-Rubioc, and J. Zubiab, "Polymers beyond standard optical fibres – fabrication of microstructured polymer optical fibres," Polym. Int. **67**(9), 1155–1163 (2018).
132. G. Barton, M. A. van Eijkelenborg, G. Henry, M. C. J. Large, and J. Zagari, "Fabrication of microstructured polymer optical fibres," Opt. Fiber Technol. **10**(4), 325–335 (2004).
133. Y. Zhang, K. Li, L. Wang, L. Ren, W. Zhao, and R. Miao, "Casting preforms for microstructured polymer optical fibre fabrication," Opt. Express **14**(12), 5541–5547 (2006).
134. W. Talataisong, R. Ismaeel, M. Beresna, and G. Brambilla, "Suspended-core microstructured polymer optical fibers and potential applications in sensing," Appl. Phys. Lett. **80**(15), 2634–2636 (2002).
135. H. Han, H. Park, M. Cho, and J. Kim, "Terahertz pulse propagation in a plastic photonic crystal fiber," Appl. Phys. Lett. **80**(15), 2634–2636 (2002).
136. Z. Liu and H.-Y. Tam, "Fabrication and sensing applications of special microstructured optical fibers," *Sel. Top. on Opt. Fib. Tech. and Appl.* vol. 2017. doi:10.5772/intechopen.70755
137. M. Goto, A. Quema, H. Takahashi, S. Ono, and N. Sarukura, "Teflon photonic crystal fiber as terahertz waveguide," Jpn. J. Appl. Phys. **43**(No. 2B), L317–L319 (2004).
138. J. Anthony, R. Leonhardt, S. G. Leon-Saval, and A. Argyros, "THz propagation in Kagome hollow-core microstructured fibers," Opt. Express **19**(19), 18470–18478 (2011).
139. A. Dupuis, J.-F. Allard, D. Morris, K. Stoeffler, C. Dubois, and M. Skorobogatiy, "Fabrication and THz loss measurements of porous subwavelength fibers using a directional coupler method," Opt. Express **17**(10), 8012–8028 (2009).
140. J. Lu, C. Yu, H. Chang, H. Chen, Y. Li, C. Pan, and C. Sun, "Terahertz air-core microstructure fiber," Appl. Phys. Lett. **92**(6), 064105 (2008).
141. M. Cho, J. Kim, H. Park, Y. Han, K. Moon, E. Jung, and H. Han, "Highly birefringent terahertz polarization maintaining plastic photonic crystal fibers," Opt. Express **16**(1), 7–12 (2008).
142. Z. Wu, J. Kinast, M. E. Gehm, and H. Xin, "Rapid and inexpensive fabrication of terahertz electromagnetic bandgap structures," Opt. Express **16**(21), 16442–16451 (2008).
143. S. Yang, X. Sheng, G. Zhao, Y. Wang, and Y. Yu, "Novel pentagram THz hollow-core anti-resonant fiber using a 3D printer," J. Infrared, Millimeter, Terahertz Waves **40**(7), 720–730 (2019).
144. T. Hidaka, H. Minamide, H. Ito, J.-I Nishizawa, K. Tamura, and S. Ichikawa, "Ferroelectric PVDF cladding terahertz waveguide," J. Lightwave Technol. **23**(8), 2469–2473 (2005).
145. L. J. Chen, H. W. Chen, T. F. Kao, J. Y. Lu, and C. K. Sun, "Low-loss subwavelength plastic fiber for terahertz waveguiding," Opt. Lett. **31**(3), 308–310 (2006).
146. D. Chen and H. Chen, "A novel low-loss Terahertz waveguide: Polymer tube," Opt. Express **18**(4), 3762–3767 (2010).
147. Md. S. Islam, J. Sultana, J. Atai, M. R. Islam, and D. Abbott, "Design and characterization of a low-loss, dispersion-flattened photonic crystal fiber for T-Ray wave propagation," Optik **145**, 398–406 (2017).
148. R. Islam, Md. S. Habib, G. K. M. Hasanuzzaman, R. Ahmad, S. Rana, and S. F. Kaijage, "Extremely high-birefringent asymmetric slotted-core photonic crystal fiber in THz regime," IEEE Photonics Technol. Lett. **27**(21), 2222–2225 (2015).
149. X. Jiang, D. Chen, and G. Hu, "Suspended hollow core fiber for terahertz wave guideing," Appl. Opt. **52**(4), 770–774 (2013).
150. Y.-F. Zhu, M.-Y. Chen, H. Wang, H.-B. Yao, Y.-K. Zhang, and J.-C. Yang, "Design and analysis of a low-loss suspended core terahertz fiber and its application to polarization splitter," IEEE Photonics J. **5**(6), 7101410 (2013).

Optics EXPRESS

151. M. Faisal and Md. S. Islam, "Extremely high birefringent terahertz fiber using a suspended elliptic core with slotted airholes," Appl. Opt. **57**(13), 3340–3347 (2018).
152. L. Vicentti and V. Setti, "Elliptical hollow core tube lattice fibers for terahertz applications," Opt. Fiber Technol. **19**(1), 31–34 (2013).
153. A. L. S. Cruz, A. C. C. Migliano, and M. A. R. Franco, "Refractive index sensor based on terahertz multimode interference fiber device," Proc. SPIE **8794**, 18794L (2013).
154. G. Hefferman, Z. Chen, L. Yuan, and T. Wei, "Phase-shifted terahertz fiber bragg grating for strain sensing with large dynamic range," IEEE Photonics Technol. Lett. **27**(15), 1649–1652 (2015).
155. Z. Chen, L. Yuan, G. Hefferman, and T. Wei, "Terahertz fiber bragg grating for distributed sensing," IEEE Photonics Technol. Lett. **27**(10), 1084–1087 (2015).
156. G. Yan, A. Markov, Y. Chinifooroshan, S. M. Tripathi, W. J. Bock, and M. Skorobogatiy, "Resonant THz sensor for paper quality monitoring using THz fiber Bragg gratings," Opt. Lett. **38**(13), 2200–2202 (2013).
157. Y. Cao, K. Nallappan, H. Guerboukha, T. Gervais, and M. Skorobogativ, "Additive manufacturing of resonant fluidic sensors based on photonic bandgap waveguides for terahertz applications," Opt. Express **27**(20), 27663–27681 (2019).
158. B. You, T.-A. Liu, J.-L. Peng, C.-L. Pan, and J.-Y. Lu, "A terahertz plastic wire based evanescent field sensor for high sensitivity liquid detection," Opt. Express **17**(23), 20675–20683 (2009).
159. B. You, J.-Y. Lu, C.-P. You, T.-A. Liu, and J.-L. Peng, "Terahertz refractive index sensors using dielectric pipe waveguides," Opt. Express **20**(6), 5858–5866 (2012).
160. B. You, J.-Y. Lu, J.-H. Liou, C.-P. Yu, H.-Z. Chen, T.-A. Liu, and J.-L. Peng, "Subwavelength film sensing based on terahertz anti-resonant reflecting hollow waveguides," Opt. Express **18**(18), 19353–19360 (2010).
161. A. Hassani and M. Skorobogatiy, "Surface Plasmon Resonance-like integrated sensor at terahertz frequencies for gaseous analytes," Opt. Express **16**(25), 20206–20214 (2008).
162. G. M. Katyba, K. I. Zaytsev, N. V. Chernomyrdin, I. A. Shikunova, G. A. Komandin, V. B. Anzin, S. P. Lebedev, I. E. Spektor, V. E. Karasik, S. O. Yurchenko, I. V. Reshetov, V. N. Kurlov, and M. Skorobogatiy, "Sapphire photonic crystal waveguides for terahertz sensing in aggressive environments," Adv. Opt. Mater. **6**, 1800573 (2018).
163. J. Sultana, Md. S. Islam, K. Ahmed, A. Dinovitser, B. W.-H. Ng, and D. Abbott, "Terahertz detection of alcohol using a photonic crystal fiber sensor," Appl. Opt. **57**(10), 2426–2433 (2018).
164. K. Ahmed, F. Ahmed, S. Roy, B. K. Paul Mst., N. Aktar, D. Vigneswaran, and Md. S. Islam, "Refractive index-based blood components sensing in terahertz spectrum," IEEE Sens. J. **19**(9), 3368–3375 (2019).
165. D. M. Mittleman, M. Gupta, R. Neelamani, R. G. Baramiuk, J. V. Rudd, and M. Koch, "Recent advances in terahertz imaging," Appl. Phys. B: Lasers Opt. **68**(6), 1085–1094 (1999).
166. J. Li, K. Nallappan, H. Guerboukha, and M. Skorobogatiy, "3D printed hollow core terahertz Bragg waveguides with defect layers for surface sensing applications," Opt. Express **25**(4), 4126–4144 (2017).
167. D. M. Mittleman, "Twenty years of terahertz imaging," Opt. Express **26**(8), 9417–9431 (2018).
168. J.-Y. Lu, C.-M. Chiu, C.-C. Kuo, C.-H. Lai, and H.-C. Chang, "Terahertz scanning imaging with a subwavelength plastic fiber," Appl. Phys. Lett. **92**(8), 084102 (2008).
169. H. Chen, W.-J. Lee, H.-Y. Huang, C.-M. Chiu, Y.-F. Tsai, T.-F. Tseng, J.-T. Lu, W.-L. Lai, and C.-K. Sun, "Performance of THz fiber-scanning near-field microscopy to diagnose breast tumors," Opt. Express **19**(20), 19523–19531 (2011).
170. C. Hua, M. Shi-Hua, Y. W.-Xing, W. X.-Mei, and W. X.-Zhou, "The diagnosis of human liver cancer by using THz fiber-scanning near-field imaging," Chin. Phys. Lett. **30**(3), 030702 (2013).
171. H. Chen, T.-H. Chen, T.-F. Tseng, J.-T. Lu, C.-C. Kuo, S.-C. Fu, W.-J. Lee, Y.-F. Tsai, Y. Y. Huang, E. Y. Chuang, Y.-J. Hwang, and C.-K. Sun, "High-sensitivity in vivo THz transmission imaging of early human breast cancer in a subcutaneous xenograft mouse model," Opt. Express **19**(22), 21552–21562 (2011).
172. A. Tuniz, K. J. Kaltenecker, B. M. Fischer, M. Walther, S. C. Fleming, A. Argyros, and B. T.Kuhlmey, "Metamaterial fibres for subdiffraction imaging and focusing at terahertz frequencies over optically long distances," Nat. Commun. **4**(1), 2706 (2013).
173. G. M. Katyba, N. V. Chernomyrdin, I. N.. Dolganova, A. A. Pronin, I. V. Minin, O. V. Minin, K. I. Zaytsev, and V. N. Kurlov, "Step-index sapphire fiber and its application in a terahertz near-field microscopy," Proc. SPIE **11164**, 11164G (2019).
174. W. Talataisong, R. Ismaeel, T. H. R. Marques, S. A. Mousavi, M. Beresna, M. A. Gouveia, S. R. Sandoghchi, T. Lee, C. M. B. Cordeiro, and G. Brambilla, "Mid-IR Hollow-core microstructured fiber drawn from a 3D printed PETG preform," Sci. Rep. **8**(1), 8113 (2018).
175. C.-H. Lai, Y.-C. Hsueh, H.-W. Chen, Y.-j. Huang, H.-c. Chang, and C.-K. Sun, "Low-index terahertz pipe waveguides," Opt. Lett. **34**(21), 3457–3459 (2009).
176. M. Mittendorff, S. Li, and T. E. Murphy, "Graphene-based waveguide-integrated terahertz modulator," ACS Photonics **4**(2), 316–321 (2017).
177. M. S. Islam, J. Sultana, C. M. B. Cordeiro, A. L. S. Cruz, A. Dinovitser, B. W.-H. Ng, and D. Abbott, "Broadband characterization of glass and polymer materials using THz-TDS," *44th Int. Conf. on Inf. Mil. and Ter. Waves (IRMMW-THz)*, DOI: 10.1109/IRMMW-THz.2019.8874013.
178. M. S. Islam, J. Sultana, C. M. B. Cordeiro, M. J.Nine, A. L. S. Cruz, A. Dinovitser, B. W.-H. Ng, H. E. Heidepriem, D. Losic, and D. Abbott, "Experimental study on glass and polymers: Determining the optimal material for potential use in terahertz technology," *IEEE Access*, (Revised version submitted).

Optics EXPRESS

179. E. V. Fedulova, M. M. Nazarov, A. A. Angeluts, M. S. Kitai, V. I. Sokolov, and A. P. Shkurinov, "Studying of dielectric properties of polymers in the terahertz frequency range," Proc. SPIE **8337**, 83370I (2012).
180. M. Naftaly and R. E. Miles, "Terahertz time-domain spectroscopy for material characterization," Proc. IEEE **95**(8), 1658–1665 (2007).
181. Z. Shi, L. Song, and T. Zhang, "Optical and electrical characterization of pure PMMA for terahertz wide-band metamaterial absorbers," J. Infrared, Millimeter, Terahertz Waves **40**(1), 80–91 (2019).
182. R. Peretti, F. Braud, E. Peytavit, E. Dubois, and J.-F. Lampin, "Broadband terahertz light–matter interaction enhancement for precise spectroscopy of thin films and micro-samples," Photonics **5**(2), 11 (2018).
183. T. Ma, K. Nallapan, H. Guerboukha, and M. Skorobogatiy, "Analog signal processing in the terahertz communication links using waveguide Bragg gratings: example of dispersion compensation," Opt. Express **25**(10), 11009–11026 (2017).
184. L. Yu, L. Hao, T. Meiqiong, H. Jiaoqi, L. Wei, D. Jinying, C. Xueping, F. Weiling, and Z. Yang, "The medical application of terahertz technology in non-invasive detection of cells and tissues: opportunities and challenges," RSC Adv. **9**(17), 9354–9363 (2019).
185. R. B. Kohlhass, A. Rehn, S. Nellen, M. Koch, M. Schell, R. J. B. Dietz, and J. C. Balzer, "Terahertz quasi time-domain spectroscopy based on telecom technology for 1550 nm," Opt. Express **25**(11), 12851–12859 (2017).